AD-A086 821 NAVAL POSTGRADUATE SCHOOL MONTEREY CA F/G 11/6
THE INFLUENCE OF PRIOR WARM ROLLING ON FRACTURE TOUGHNESS OF HE--ETC(U)
MAR 80 J F MCCAULEY

UNCLASSIFIED NL

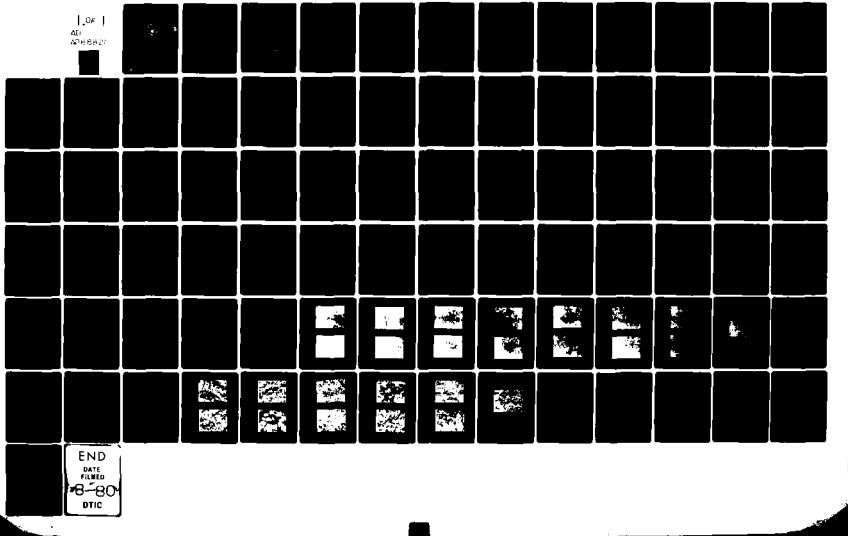

END
DATE FILMED
8-80
DTIC

LEVEL II

NAVAL POSTGRADUATE SCHOOL

Monterey, California

THESIS

THE INFLUENCE OF PRIOR WARM ROLLING ON FRACTURE TOUGHNESS OF HEAT TREATED AISI 52100 STEEL.

by

Jeffrey F. McCauley

March 1980

Thesis Advisor: T. R. McNelly

Approved for public release; distribution unlimited

Unclassified

SECURITY CLASSIFICATION OF THIS PAGE (When Data Entered)

REPORT DOCUMENTATION PAGE	READ INSTRUCTIONS BEFORE COMPLETING FORM
1. REPORT NUMBER	2. GOVT ACCESSION NO. AD-A086821 / 3. RECIPIENT'S CATALOG NUMBER
4. TITLE (and Subtitle) The Influence Of Prior Warm Rolling On Fracture Toughness Of Heat Treated AISI 52100 Steel	5. TYPE OF REPORT & PERIOD COVERED Master's Thesis March 1980 / 6. PERFORMING ORG. REPORT NUMBER
7. AUTHOR(s) Jeffrey F. McCauley	8. CONTRACT OR GRANT NUMBER(s)
9. PERFORMING ORGANIZATION NAME AND ADDRESS Naval Postgraduate School Monterey, California 93940	10. PROGRAM ELEMENT, PROJECT, TASK AREA & WORK UNIT NUMBERS
11. CONTROLLING OFFICE NAME AND ADDRESS Naval Postgraduate School Monterey, California 93940	12. REPORT DATE March 1980 / 13. NUMBER OF PAGES 82
14. MONITORING AGENCY NAME & ADDRESS(if different from Controlling Office)	15. SECURITY CLASS. (of this report) Unclassified / 15a. DECLASSIFICATION/DOWNGRADING SCHEDULE
16. DISTRIBUTION STATEMENT (of this Report) Approved for public release; distribution unlimited.	
17. DISTRIBUTION STATEMENT (of the abstract entered in Block 20, if different from Report)	
18. SUPPLEMENTARY NOTES	
19. KEY WORDS (Continue on reverse side if necessary and identify by block number) Fracture Toughness Ultra High Carbon Steel	
20. ABSTRACT (Continue on reverse side if necessary and identify by block number) An investigation was conducted to determine the effects of prior warm rolling on AISI 52100 bearing steel in the hardened condition. Microstructural and mechanical properties of both standard and warm rolled 52100 were investigated. Heat treatments, consisting of both conventional hardening treatments and isothermal transformation treatments, were conducted prior to fracture toughness, hardness, and tensile testing. Conventional hardening treatments resulted in martensitic → over	

DD FORM 1 JAN 73 1473 (Page 1) EDITION OF 1 NOV 65 IS OBSOLETE S/N 0102-014-6601

Unclassified

SECURITY CLASSIFICATION OF THIS PAGE (When Data Entered)

Block 20 continued...

structures with low toughness; prior warm rolling resulted in the rolled materials exhibiting both higher hardness and toughness than the standard 52100 in the hardened condition. Isothermal transformation treatments resulted in substantially improved toughness, especially in the material processed at 300 C.

APPROVED FOR PUBLIC RELEASE; DISTRIBUTION UNLIMITED

The Influence Of Prior Warm Rolling On Fracture Toughness Of Heat Treated AISI 52100 Steel

by

Jeffrey F. McCauley
Lieutenant, United States Navy
B.S., University Of Kansas, 1975

Submitted In Partial Fulfillment Of The
Requirements For The Degree Of

MASTER OF SCIENCE IN MECHANICAL ENGINEERING

from the

NAVAL POSTGRADUATE SCHOOL
March 1980

Author _____

Approved by: _____
Thesis Advisor

_____
Second Reader

_____
Chairman, Department Of Mechanical Engineering

_____
Dean Of Science And Engineering

ABSTRACT

An investigation was conducted to determine the effects of prior warm rolling on AISI 52100 bearing steel in the hardened condition. Microstructural and mechanical properties of both standard and warm rolled 52100 were investigated. Heat treatments, consisting of both conventional hardening treatments and isothermal transformation treatments, were conducted prior to fracture toughness, hardness, and tensile testing. Conventional hardening treatments resulted in martensitic structures with low toughness; prior warm rolling resulted in the rolled materials exhibiting both higher hardness and toughness than the standard 52100 in the hardened condition. Isothermal transformation treatments resulted in substantially improved toughness, especially in the material processed at 300 C.

TABLE OF CONTENTS

LIST OF TABLES

LIST OF FIGURES

ACKNOWLEDGEMENT

I wish to express my appreciation to Professor Terry R. McNelly for his guidance and assistance, to Professor Donald Boone for his assistance, to Mr. Tom Kellog and Mr. Ken Mothersell for their support, and to Dianne, Chris, Jeff Jr., and Kerry for their patience.

I. INTRODUCTION

A. PURPOSE

The purpose of this research was to investigate the effects of extensive warm rolling prior to hardening on the fracture toughness of AISI 52100 steel in the hardened condition. This effort was part of ongoing research at the Naval Postgraduate School (NPS) into the mechanical properties of high-carbon and ultra-high carbon steels. This work follows that of Taylor [Ref. 1] who determined that warm rolled 52100 steel performed better in fracture toughness testing than other ultra-high carbon (UHC) steels tested. The 52100 steel was tested in accordance with the American Society for Testing and Materials (ASTM) Standard E399-78 [Ref. 2] to determine the processing effects on the materials resistance to unstable crack propagation. The ultimate goal of this research was to determine if microstructural changes resulting from extensive warm rolling prior to hardening persist through subsequent heat treatments, and if these microstructural changes influence the fracture toughness and hardness of the material. It is believed that these determinations will assist in the eventual use of this warm rolling process for the production of an improved bearing material.

B. BACKGROUND

At the beginning of this century, Stribeck recognized that a low allow chromium steel proved to be particularly

adaptable for use in anti-friction roller bearings [Ref. 3]. In subsequent years, investigation carried out by bearing manufacturers led to the standardization of different materials for bearing use, including AISI 52100 steel, which has been used by the bearing industry since the 1920's. This material is high in chromium and carbon content, and is characterized by high hardness and excellent wear resistance [Ref. 4].

The suitability of a steel for high local cyclic stressing, required for all roller bearing use, has been shown to be insufficiently predictable only on the basis of chemical content and the values of static strength, since the endurance strength is decidely influenced by possible inhomogeneities and grain texture. As discussed in Ref. 5, ball and roller bearing steel must not exhibit macroscopic defects such as cavities, blowholes, and internal fissures. They must also be free from non-metallic inclusions and segregation from which microcracks can initiate and ultimately result in failure of the bearing. The type, size, and number of these inclusions depend on the melting and processing procedures. Further quality requirements are a fine grain structure and fine uniformly distributed carbides. Material processing has consistently improved over the years in an effort to meet these quality requirements. Vacuum induction melting has been used to minimize dissolved gas content and to better control other impurities. However, a refractory crucible is used in the induction melting porcess, with the result that sometimes refractory particles get into the melt. Research by Morrison, Walp, and

Remorenko [Ref. 6] in the late 1950's suggested this explanation for their observation that consumable electrode vacuum arc melting procedures resulted in consistently higher quality bearings with longer fatigue lives. The present day procedure involves vacuum induction melting followed by consumable electrode vacuum arc remelting. In the consumable electrode vacuum melting process, the ingot is used as one terminal of the arc, and the process is completely clean resulting in few impurities or inclusions and a more uniform structure. As a result, the reliability of bearings has been improved.

Even with the improved processing techniques, undissolved carbides continue to be a problem, as pointed out by Kar, Horn and Zackay in Ref. 7:

> "Commercial use of 52100 steel involves incomplete austenitization at relatively low temperatures, resulting in incomplete dissolution of alloy carbides, predominately Fe-Cr complexes. It is well known that undissolved carbides cause poor toughness."

As 52100 is cooled from its normal austenitizing temperature, 850°C, undissolved carbide particles usually remain in the microstructure. These particles are brittle and act as crack nucleation sites, and also offer a preferred path for crack propagation through the material, resulting in the reduced fracture toughness. In bearing applications, under high contact (Hertzian) stresses, coarse undissolved carbides result in subsurface cracks which can propagate to the surface

sulting in failure due to spalling. Kar also points out that these carbides can be dissolved more completely by increasing the austenitization temperature [Ref. 7]. This, however, creates a new set of problems. The higher processing temperature results in larger austenite grain size. Upon quenching, these large grains form coarse martensite with increased stress concentrations and still worse fracture toughness. Also, retained austenite becomes a problem and quench cracking, due to the coarse martensite, becomes severe. Furthermore, the increased stresses involved in the martensite transformation for the larger grained material causes a depression of the martensite start temperature, again adding to the increased possibility of quench cracking as discussed in Ref. 8.

Professor Oleg D. Sherby of Stanford University's Department of Material Science and Engineering discovered that by extensively warm rolling an ultra-high carbon steel while cooling through the austenite plus carbide region of the phase diagram, it is possible to break up grain boundary carbide networks which could otherwise form [Ref. 9] Further warm rolling below the eutectoid transforms additional carbides formed from the decomposing austenite to a very fine, spheroidized condition. This thermomechanical processing results in a fine spheroidal carbide distribution in a fine ferrite matrix in the as rolled condition. The end product is a steel that has good strength and ductility. This also suggests a possible solution to the carbide problem in 52100

bearing steel. If the carbides are very fine prior to austenitizing, the standard hardening treatment can more completely dissolve them. Any carbides retained would be less detrimental due to their reduced size. Ultra-high carbon steels, the focus of Sherby's work, are generally considered to be steels with between 1.1 and 2.0 weight percent carbon. AISI 52100 steel, with 1.0 weight percent carbon is more commonly referred to as a high carbon steel, but the material meets the requirements for superplastic flow required for the Sherby process as detailed in Ref.9.

C. PREVIOUS RESEARCH

The research at NPS initially focused on AISI 52100 steel, tested by Leiutenant Commander William Goesling [Ref. 10] to determine its suitability for use as an armor material. In this first effort, test results indicated that 52100 steel, processed by the Sherby method, compared favorably in the as rolled condition with existing armor materials. Lieutenant Commander Donald Rowe and Captain Douglas Hamilton [Ref. 11] continued examining the terminal ballistic characteristics of this material, but in the hardened conditon. They found that the heat treated material displayed substantially reduced penetration resistance after heat treatment. The ballistic research was expanded by Lieutenants Ronald Martin and James Phillips [Ref. 12]. Tests showed that 52100, processed by the Sherby method, display a reduced tendency to form adiabatic shear bands than did currently used armor materials. Adiabatic shear bands are associated with

reduced resistance to penetration. Again, as rolled 52100 was found to be superior to conventional armors. Lieutenant Commander Randy Hillier increased the scope of the ballistic research to include untra-high carbon steel alloys containing 1.5 percent carbon. As pointed out in Ref. 13, none of these steels was found to have ballistic characteristics as good as 52100.

Lieutenant Commander James Taylor initiated research at NPS into more fundamental mechanical properties of 52100 steel, including fracture toughness. After testing various ultra high carbon steels as well as 52100, it was noted in Ref. 1 that 52100 was the only material tested that showed refined carbides after rolling by the Sherby process. It was further found that 52100 steel exhibited substantially higher fracture toughness in the as-rolled condition as compared with the other steels tested. Commander Iksik Chung continued to investigate properties of 52100. As described in Ref. 14 this warm rolled 52100 material was found to have improved fatigue resistance, particularly after heat treatment involving isothermal transformation subsequent to austenitizing. Lieutenant Clarence Schultz has conducted an as yet unpublished investigation into the effect of various austenitization times and temperatures on the hardness of 52100, both in conventional and in warm-rolled material. Results indicate that the rolled material exhibits a consistently higher hardness and more rapid hardening response than conventional material after identical hardening treatments.

II. REVIEW

A. THE SHERBY WARM ROLLING PROCESS

Professor Oleg D. Sherby at Stanford University has investigated warm rolling as a process to develop a fine, spheroidized structure in high carbon steels as explained in Ref. 15. It is well known that pearlitic microstructures in steel will spheroidize when heated to just under the eutectoid temperature (Fig. 1). This spheroidizing anneal softens the steel by breaking down the lamellar pearlitic structure, resulting in a more stable grain structure. The carbides become spheroidal particles in a ferrite matrix. The rate of spheroidization is controlled by diffusion and is relatively slow. Sherby has established that concurrent plastic deformation during this spheroidize annealing dramatically increases the rate of spheroidization, results in relatively fine spheroidal carbides and in a refined ferrite matrix, and that still finer spheroid particles can be formed by increasing the strain rate or reducing the temperature of deformation.

Sherby and Walser [Ref. 16] found in later research that high and ultra high carbon steels may display superplasticity, with elongations up to 700 percent, at warm temperatures. A process was developed to utilize this characteristic for grain refinement. Research conducted at Stanford has shown this thermomechanical process is capable of developing composites of cementite (iron carbide, Fe_3C) in ferrite with ferrite grains as small as one micron in size, and cementite finer

than 0.1 micron in size. Just as significant, this was accomplished with no cracking and a minimal amount of energy expended in the rolling process due to the superplasticity. The result of this research was a strong and ductile material.

As a prerequisite to superplasticity behavior, the material must have fine, equiaxed grains of two phases, each phase having apprixomately the same strength at the deformation temperature. Sherby has defined a superplastic material as one whose strain rate sensitivity coefficient is greater than 0.4, and which is capable of elongation of at least 500 percent. The primary mechanism for superplastic deformation is diffusion-accomodated grain boundary sliding [Ref. 16].

Although Sherby's research has focused on materials with from 1.3 to 2.3 weight percent carbon, the process has been found to be applicable to AISI 52100 steel [Ref. 17]. Indeed, superplasticity in this 52100 steel suggests ease of manufacture of components such as bearings by warm rolling or forging under superplastic conditions. The accompanying fine microstructure, especially the refined carbides, will also contribute to improved toughness in the subsequent hardened conditions of the material.

B. FRACTURE TOUGHNESS THEORY

Fracture toughness is defined as that property of a material resisting the extension of an existing crack [Ref. 17]. Crack extension consists of three separate stages: (1) initial subcritical propagation, (2) transition from slow to rapid propagation, and (3) fast fracture. As pointed out

by Tom [Ref. 18], "the first and third stages may be considered steady state phenomena" in that the rate of crack propagation is directly proportional to the load applied and the crack length. The second stage occurs abruptly when a critical crack size and stress is attained. It is at this critical condition that fracture toughness measurement is important. The fracture behavior of a given material depends also on the mechanical properties of that material, and the mechanism by which the fracture proceeds to completion [Ref. 19].

Griffith was the first to suggest a quantitative relationship to describe fracture via crack propagation, as discussed in Refs. 1,18 & 19. It was proposed that unstable crack extension would occur if the rate of release of elastic strain energy was greater than the rate of increase in surface energy associated with the presence of a growing crack. The Griffith analysis worked well for modelling perfectly elastic material. It failed, however, to account for work done during any plastic deformation prior to crack extension. Irwin improved the Griffith analysis by adding to the energy balance a parameter including this work. Continued research by Irwin showed that the energy approach could be simplified to allow specimen geometry effects and loading effects to be described in terms of a single parameter, the stress intensity factor, K_I. Tom defines the stress intensity factor [Ref. 18], "as a parameter that reflects the redistribution of stress in a body resulting from the introduction of a crack". Its

magnitude is a function of the gemetry of the sample, the size and location of the crack, and the loading of the sample. Tests indicated [Ref. 19] that the critical stress intensity at the crack tip for fast fracture was dependent on sample thickness up to a certain minimum thickness. After this thickness was exceeded, tests gave a constant stress intensity value indicating this value could be considered a material property. This value is designated K_{Ic}. The Griffith-Irwin theory was used in investigating the stress distribution at a crack tip to explain the apparent dependence on thickness. The stress fields near a crack tip are of three basic types, as shown in Fig. 2. As defined in Ref. 19, the modes are:

Mode I. Opening or tensile mode, where the crack surfaces move directly apart.

Mode II. Sliding or in-plane shear, where crack surfaces slide over one another in a direction perpendicular to the leading edge of the crack.

Mode III. Tearing or anti-plane shear mode, where the crack surfaces move relative to one another and parallel to the leading edge of the crack.

Mode I type of crack surface displacements have been found to be the most prevalent mode of fracture in engineering situations. As a consequence, methods used to quantify K_I for stress-crack relationships have focused on this mode. For the notation shown in Fig. 3, the crack tip stresses are found to be

$$\sigma_y = \frac{K}{\sqrt{2\pi r}} \cos\frac{\theta}{2}\left(1 + \sin\frac{\theta}{2}\sin\frac{3\theta}{2}\right)$$

$$\sigma_x = \frac{K}{\sqrt{2\pi r}} \cos\frac{\theta}{2}\left(1 - \sin\frac{\theta}{2}\sin\frac{3\theta}{2}\right)$$

$$\tau_{xy} = \frac{K}{\sqrt{2\pi r}} \left(\sin\frac{\theta}{2}\cos\frac{\theta}{2}\cos\frac{3\theta}{2}\right)$$

where

K_I = stress intensity factor.

σ_x = normal stress component in x direction.

σ_y = normal stress component in y direction.

τ_{xy} = shear stress component in the plane perpendicular to the x direction acting in the y direction.

$r\varepsilon\theta$ = popular coordinates relative to the crack tip.

It is apparent that as r approaches zero, these stresses become very large. This does not happen because of the onset of plastic deformation in the vicinity of the crack tip. A plastic zone forms around the crack tip, embedded within a large region of material which is still elastic. This plastic region is acted upon by either biaxial ($\sigma_x+\sigma_y$) or triaxial ($\sigma_x+\sigma_y+\sigma_z$) stresses that control the extent of plastic straining in the region. If the sample is relatively thin, a biaxial stress state will exist at the crack tip. This

circumstance arises since the elastic material outside the plastic zone exerts little restraining effect on deformation in the z, or thickness, direction; for Mode I, surfaces normal to z are assumed to be fraction free and thus σ_z tends to zero and a biaxial state exists. This condition is defined as plane stress.

In thick sections, a stress is developed in the thickness (z) direction:

$$\sigma_z = \nu(\sigma_x+\sigma_y)$$

This stress arises since elastic material outside the plastic zone now restrains deformation in the z direction and thus $\varepsilon_z = 0$. A condition of triaxial stress exists at the crack tip. This condition is defined as plane strain since $\varepsilon_z = 0$ and the strains are now biaxial $(\varepsilon_x+\varepsilon_y)$. The size of the plastic zone at the crack tip has been found to depend on the yield strength of the material (σ_{ys}), the stress intensity factor (K), and the condition of loading. The radius of the plastic zone (r_y) is defined as

$$r_y = \frac{1}{2} (K/\sigma_{ys})^2 \qquad \text{(for plane stress)}$$

$$r_y = \frac{1}{6} (K/\sigma_{ys})^2 \qquad \text{(for plane strain)}$$

It is clear the plane strain condition results in a smaller plastic zone at the crack tip. It follows that the plane strain condition exhibits a smaller critical stress intensity factor since less total energy is requred for plastic

deformation prior to crack extension. In a thinner section, plastic zone constraint is less, more work is done in plastic deformation prior to crack extension, and therefore a higher stress intensity factor is indicated.

When the stress intensity factor increases to the point that causes fast fracture, the value is referred to as the critical stress intensity factor or fracture toughness, (K_c). K_c will vary with thickness for reasons described above. As the thickness increases, toughness drops until it reaches a lower bound referred to as the plane strain fracture toughness (K_{IC}), as noted previously. The plain strain fracture toughness is a material property, and is used in predicting the fracture behavior of a material.

As noted above, the plastic zone size is a function of the loading condition; it is also a function of the yield strength of the material, being smaller the higher the yield strength. Also, the smaller the plastic zone size at which fast crack growth occurs, the more the loading conditions tend toward plane strain. It follows, then, that the thickness at which a material will exhibit plane strain behavor decreases as yield strength increases. The significance of this point will become clear later in consideration of data obtained in this study.

C. MATERIAL HISTORY

The AISI 52100 steels tested for this research were received from two sources. The alloy content of each is indicated in Table 1. The materials designated "550 C Rolled"

and "650 C Rolled" were fabricated from a commercial grade steel obtained from Vasco Pacific Steel Company. The material was received in the form of cylindrical bars 7.9 cm in diameter that were vacuum induction melted, consumable electrode vacuum arc remelted, hot rolled and heat treated as described in chapter one. The material was then processed at Viking; two ten inch lengths of this 52100 steel were austenitized at 1000°C for three hours. Each was then forged to 7.6 cm x 5.1 cm x length plates and air cooled to a temperature below 400°C. These plates were then reheated to 550 C or 650 C, respectively, and warm rolled, reheating between each pass, from 5.1 cm to final thickness at a rate of 0.13 cm per pass. The 550 C material had an average final thickness of 0.81 cm. The 650 C rolled material had an average final thickness of 0.76 cm. The material was then air cooled to ambient temperature. The material designated "Standard 52100" was a commercial grade steel received from Carpenter Steel Company as a cylindrical bar 7.9 cm in diameter, processed in the same manner as before.

Fracture toughness specimens were machined from the rolled and standard materials to the dimensions indicated in Fig. 4. The specimens from the rolled material were cut with transverse-longitudinal (T-L) orientation as illustrated in Fig. 5. Some variation in thickness (B) was experienced due to the rolling. Various hardening treatments were subsequently performed as described in Table 2, and schematically illustrated in Figs. 6 and 7. After the fracture toughness

samples were in the hardened condition, they were cut to a depth of 0.71 cm using a Douvall diamond cut off wheel, 0.08 cm in width. The crack initiation notch was then machined to a root radius of 0.0076 cm (0.003 in) using an Electro-Discharge Machine (EDM) at the Lawrence Berkeley Laboratory for Molecular and Materials Research.

D. EXPERIMENTAL PROCEDURES

1. Fracture Toughness Testing

The three point bend specimens used for fracture toughness testing were designed according to the specifications outlined in ASTM E399-78, Standard Test Method for Plane Strain Fracture Toughness of Metallic Materials [Ref. 2]. It was not possible to fatigue precrack the steel in the quenched and tempered condition (heat treatments 1 and 2, Table 2). Consequently, tests were conducted using a machined crack having a root radius of 0.0076 cm (0.003 in) for all conditions. This method was suggested by Heald, Spinks, and Worthington [Ref. 21], and recommended by Kar, Zackay, and Horn [Ref. 7], who experienced the same difficulty in fatigue precracking hardened 52100 steel. ASTM E399 dictated that the total crack length measure between 0.45W and 0.55W (Fig. 4).

The fracture toughness tests were conducted on a Series 810 Materials Testing System (MTS) Model 976.01-3 servo hydraulic test machine using loading apparatus designed by Taylor and fully described in Ref. 1. The specimens were

placed on hardened steel dowel pins 0.32 cm in diameter and loaded by a fixture with 0.48 cm radius at point of contact. Positioning was such as to create the loading condition as indicated in Fig. 8.

An MTS Model 632.20B clip gage was used for measuring crack opening displacement. A pair of knife edges were bonded to the fracture toughness specimen, and the gage was clipped to these edges with a gage length of 0.44 cm. The gage was calibrated by MTS Corporation in March 1979, and a range card was provided by MTS to ensure compatibility between the gage and the Model 440.21 Transducer Signal Conditioner. Calibration was checked prior to each series of tests to ensure accuracy of both the gage and the load cell of the MTS Series 810 system.

Fracture toughness tests were conducted by loading the specimen to failure using an inverted ramp signal from the function generator under stroke control at the rate of 0.013 cm/min. A Hewlett Packard plotter was used to provide a graphic record of load versus crack opening displacement. A second plotter was used to record loading rate to ensure that the stress intensity factor rate of increase was maintained between 0.55 and 2.75 $MPa \cdot m^{1/2}$ per second as required by the standard.

The apparent fracture toughness (K_Q) is the measured value of stress intensity factor sufficient to cause failure. This value was calculated as

$$K_Q = \frac{P_Q S}{BW^{3/4}} \times f\left(\frac{a}{w}\right)$$

where

$$f\left(\frac{a}{w}\right) = \frac{3(a/w)^{1/2}(1.99-a/w(1-a/w)(2.15-3.99a/w+2.7(a/w)^2)}{2(1+2a/w)(1-a/w)^{3/2}}$$

The parameters B, S, W, and a are as indicated in Fig. 8. The load P_Q is determined in accordance with Ref. 2. Basically, there are three methods of measuring P_Q depending on the nature of the load versus displacement data, as indicated in Fig. 9. In this effort, all failures were type-three failures.

2. Mechanical Testing

After fracture toughness tests were conducted, each sample was tested for hardness using a Wilson Model 1 JR Rockwell Hardness Tester. The hardness of the material was determined avaraging no less than eight individual hardness tests. All tests were conducted at room temperature.

Tensile tests were conducted on materials given isothermal heat treatments (treatments 3 and 4, Table 2). The tests were conducted on the MTS Model 810 using tensile grips with the capacity to load the specimen to 242MPa. The tensile samples were loaded to failure using a ramp function from the function generator in stroke control at a rate of 0.21 cm/min. Load versus time was recorded in a Hewlett Packard strip chart recorder.

3. Microscopy

Microstructural features were investigated from samples of each material. Each sample was examined at 1000X on a Bausch and Lomb Balpan Microscope after polishing and etching using a two percent Nital etchant. Fracture surfaces were examined using a Cambridge Scientific Instruments Limited S 4-10 Stereoscan Scanning Electron Microscope. Retained austenite was determined with a Picker X-ray Diffractometer using the spectrometer method discussed by Ogilvie in Ref. 22.

III. RESULTS/DISCUSSION

A. MICROSTRUCTURAL ANALYSIS

Figures 10-12 illustrate the microstructure of the standard 52100, 650°C rolled, and 550°C rolled materials, all at 1000 diameters. The standard 52100 (Fig. 10) exhibits a ferrite matrix with coarse spheroidized Fe-Cr-C carbides present in a non-uniform distribution. These carbides, when incompletely dissolved during hardening treatment, reduce fatigue life in bearings. Figure 11 illustrates the 52100 material processed by the Sherby rolling method at 650°C. The increased degree of homogeneity is apparent; the carbides are finer and more uniformly dispersed as compared to the standard 52100. Figure 12 shows that rolling at 550°C was less successful in breaking up the carbides than rolling at 650°C. Note some coarser carbides present as compared to Fig. 11, but finer as compared to the standard material in Fig. 10. It is apparent from these micrographs that the Sherby rolling method resulted in a more uniform, refined distribution of carbides. Also, a characteristic of this processing procedure is refinement of the ferrite matrix grain size.

1. 775-ST and 850-ST

Figures 13-18 show at 1000 diameters magnification the microstructures resulting from quenching and tempering, using two different hardening temperatures. For the 775-ST treatment, all materials showed a tempered martensitic structure with numerous carbides not in solution as a result of the relatively low austenitizing temperature.

The grain refinement resulting from the Sherby process persisted through these heat treatments, as the standard material exhibits a substantially coarser structure. Large undissolved carbides are present in the standard material as seen in Figs. 12 and 15. Finer carbides, more uniformly dispersed, are present in the 650°C and 550°C rolled materials as seen in Figs. 14, 15, 17, and 18. Note that the grain size in the 650 C rolled material (Figs. 14 and 17) appear to be slightly finer than that in the 550 C rolled material (Figs. 15 and 18).

2. 250-IT and 300-IT

Quenching a material to a temperature just above the martensite start temperature results in the formation of bainite, a structure lower in hardness and higher in toughness. The isothermal transformation of these materials at the two holding temperatures investigated resulted in widely varied microstructures. All materials were austenitized at 850°C prior to the isothermal hold at either 250°C or 300°C.

After the 250°C isothermal transformation, the standard 52100 material consisted primarily of a bainitic structure with some martensite also present (Fig. 19). Undissolved carbides are readily apparent, as is the lack of homogeneity in their distribution. The rolled materials (Figs. 20 and 21) have martensite, some bainite, and retained austenite with very few undissolved carbides in evidence. It is important to note here that these are the only structures in which any retained austenite was found. The difference in grain size

between the 650°C and 550°C rolled materials is more pronounced. It is likely that 250 C is below the martensite start temperature (M_s) for the rolled materials. Retained austenite, present in the rolled materials but not in the standard material, and the apparent presence of martensite indicate that the rolled materials are below M_s. The bainitic microstructure and the absence of retained austenite indicate that the standard material is above M_s.

The 300°C transformation temperature, on the other hand, was above the martensite start temperatures for all materials. Again, the standard 52100 (Fig. 22) material exhibited primarily bainite, and perhaps even some pearlite. Coarse carbides are again in evidence. The rolled materials show little evidence of undissolved carbides. The 650°C rolled material maintained its fine grain size (Fig. 23) and degree of homogeneity in transforming to bainite. The 550°C rolled material, shown in Fig. 24, is believed to be a primarily bainitic structure, but the exact metamorphosis of this relatively coarse structure from previously observed fine microstructures cannot be fully explained. The material at least appears to have undergone some grain growth.

B. FRACTURE TOUGHNESS TEST RESULTS

The major goal of this research effort was to measure the fracture toughness of these materials after heat treatment. The procedures for conducting these tests have already been described. The corolation between the apparent fracture

toughness (K_Q) obtained using a notched specimen and the plane strain fracture toughness (K_{IC}) is a function of the notch root radius, the total crack length, and the ultimate tensile strength of the material. This relationship is based on the work of Heald, Spink, and Worthington [Ref. 21] and is described in more detail in Appendix A. The focus of this research was on the relative toughness of the rolled materials as compared to the standard 52100 material for the same geometry and the same heat treatment. These comparisons can be made without ambiguity using the measured apparent fracture toughness (K_Q).

1. 775-ST and 850-ST

The fracture toughness testing results for the materials subjected to standard hardening treatments are contained in Table 3. Hardness was also measured using the Rockwell C scale, and the results are included in Table 3. Figs. 25 and 26 are graphical representations of the fracture toughness and hardness (respectively) versus austenitizing temperature for these two heat treatments.

For both austenitizing temperatures, the fracture toughness of the rolled materials was consistently higher than the standard 52100. The higher austenitizing temperatures resulted in lower toughness but higher hardness for all materials tested.

The average hardness values indicate that the 550°C rolled material was lower in hardness as compared to the standard material, while the 650°C rolled material was

slightly higher. However, the standard deviation of the measured hardnesses at the 775 C austenitizing temperature was large, $0.7R_c$. Thus, the only conclusion that can be made from this data is that the hardnesses are essentially equal. At the higher austenitizing temperature , both the rolled materials were consistently higher in hardness than the standard material, and the standard deviation for the hardness measurements was very low, $0.2R_c$.

In analyzing these results, it is important to understand the effect of the austenitizing temperature on the amount of carbon in solution, and the effect of increased carbon content or martensite. The hardness of martensite increases with carbon content. The amount and homogeneity of the distribution of carbon in the martensite is dependent on austenitizing time and temperature. At the lower austenitizing temperature, there was both less carbon in solution and lesser degree of diffusion of carbon, resulting in the lower hardness. At the higher austenitizing temperature, more carbon went into solution and in a more uniform distribution, resulting in higher hardness. This high carbon content in the martensite also accounts for the lower fracture toughness for all materials tested at the higher austenitizing temperature. The harder the martensite, the more brittle it is; therefore, lower toughness results.

The higher hardness of the rolled material, in conjunction with the higher fracture toughness relative to the standard material indicates a significant combination. As

a general rule, toughness is inversely proportional to hardness. Here it was found that the rolled material exhibited both higher hardness and toughness than the standard material. The fine grain size and finer, more completely dissolved carbides increased the toughness. By more completely dissolving the carbides, more carbon was in solution, increasing the hardness; the refined grain size may also contribute to increased hardness. This result suggests both improved fatigue life and increased wear resistance for roller bearings.

2. 250-IT and 300-IT

Research conducted at the University of California, Berkeley, determined that isothermal transformation of the standard material at 250°C improved the fracture toughness. As previously discussed, this process leads to the formation of bainite, which has lower hardness but higher toughness that martensite. While the standard 52100 material is known to have a martensite start temperature of approximately 250 C, the start temperature for the rolled material is not known. The fine grain size of the rolled material would raise the martensite start temperature, but to what specific value has not yet been determined.

To investigate the effect of isothermal transformation on the rolled materials, two holding temperatures were used as indicated in Table 2, treatments 3 and 4, prior to fracture toughness testing. Results of these tests are tabulated in Table 4, and graphically represented in Figs. 27 and 28.

At the 250° C transformation temperature, the standard material possessed significantly higher fracture toughness than the rolled material. Since 250° C is above the martensite start temperature for the standard material, but below for the rolled material, this was not unexpected. The hardness of the rolled material is slightly higher than the standard material, but not enough to fully explain the difference in fracture toughness values. This difference could be caused by the retained austenite in the rolled material. As pointed out in the microstructural analysis section, this was the only material found to have retained austenite; the standard material had no measurable amount of austenite. This retained austenite, under stress, can transform to brittle martensite and result in a more brittle failure (Ref. 19).

Fracture toughness values for the rolled materials were substantially higher for the samples isothermally transformed at 300° C. The standard material, however, displayed a reduced fracture toughness. The 300° C holding temperature was clearly above the martensite start temperature for the rolled material, and consequently an increase in fracture toughness resulted. The standard material suffered an embrittling effect that can be attributed to cementite formation at prior austenitic grain boundaries. This embrittlement, similar to temper embrittlement, is more fully explained by Hertzberg in Ref. 19. Since the standard 52100 material has larger austenitic grains, relatively little cementite film need be present to lead to relatively brittle failure. The fracture toughness of the rolled materials clearly

indicate that the finer grain size prevented this embrittlement in the rolled materials. The 550° C rolled material and the standard 52100 were very close in hardness at R_c53.5. The 650° C rolled material was significantly lower than both of these, R_c50.5.

C. SCANNING ELECTRON MICROSCOPY

Subsequent to the fracture toughness testing, the fracture surfaces of each material was investigated for each heat treatment with the following result:

1. 775-ST and 850-ST

The fracture surfaces of the material given the conventional hardening heat treatments are shown in Figs. 29-34, at 2000 diameters magnification. The fractographs for the 775-ST treatment are shown in Figs. 29-31. The successive decrease in cleavage facets and dimples from Fig. 29 to Fig. 30 to Fig. 31 indicates decreasing size of the acicular needles of martensite as a result of the different degrees of grain refinement.

Fractographs of the 850-ST heat treatments are pictured in Figs. 32-34. In this series, the variation in grain size is more prouounced. The flat surfaces shown in Fig. 32 are indicative of a low-energy, brittle fracture. Carbide particles can be seen on these flat surfaces. These particles offer a preferred path for propagation, greatly reducing the resistance to crack propagation in the material. This fracture is a 95% brittle, intergranular-cleavage fracture. The rolled materials, on the other hand, show some dimples and small cleavage facets in martensite platelets, indicative

of a higher energy quasi-cleavage failure. These fractographs then, indicate that the rolled materials would display higher fracture toughness than the standard 52100 material, and corroborate the results obtained in the fracture toughness tests.

2. 250-IT and 300-IT

For the 250° C isothermal transformation treatment, no discernable difference was found between the fracture surfaces of the 650° C rolled and the 550° C rolled materials. Depicted in Fig. 35 is the fracture surface of the standard material at 2000 diameters magnification. Note the increased number of dimples as compared to the material with a standard quench and temper following austenitization at the same 850° C temperature. These dimples, formed by microvoid coalescence, are indicative of plastic deformation due to the more ductile nature of bainite. Figure 36, showing the 550°C C rolled material, exhibits far fewer dimples and a preponderance of clevage facets, indicative of lower toughness.

The difference in fracture surface appearance from those given the 250-IT heat treatment to those given the 300-IT treatment was significant. The standard material, which showed increased ductility after the 250°C isothermal transformation exhibits now a brittle fracture surface after the 300°C isothermal transformation. As shown in Fig. 37, the fracture surface contains large cleavage facets separated by tear ridges. This is a result of the embrittlement caused by cementite formation at prior austenitic grain boundaries previously discussed. The 550°C rolled material exhibited

large dimples and very few cleavage facets (Fig. 38). The fracture surface would indicate a coarser bainitic structure than the 250°C transformed material. The 650 rolled material shown in Fig. 39, however, indicates a large number of smaller dimples, indicating a finer grain size. The fracture surface of both rolled materials indicate substantially higher ductility than the standard material for this heat treatment. Here again, the fracture surface appearances corroborate and help to explain the results obtained in the fracture toughness tests.

D. OVERVIEW

Figure 40 graphically displays the fracture toughness values obtained for the variously processed 52100 steels. It is clearly evident that the material rolled according to the Sherby process exhibits a consistently higher fracture toughness after comparable heat treatments. For the isothermal transformation treatment, the fracture toughness values to be compared should be the rolled material at the 300°C transformation temperature and the standard material at the 250°C holding temperature, due to the difference in martensite start temperature.

An important repationship to investigate in looking at fracture toughness is the toughness-hardness relationship. Figures 41 and 42 show the fracture toughness determined in these tests as a function of hardness. There are two significant results. First, at the 850°C austenitizing temperature, both higher toughness and hardness was attained for both

rolled materials when compared to the standard material. Secondly, at the other end of the scale, the 550°C rolled material showed a substantially higher toughness at the same hardness as the standard material.

These results offer come intriguing possibilities. It is possible the Sherby rolling process can be utilized to not only increase the hardness and toughness of fully hardened 52100 steel by reducing carbide size, but may alleviate the temper embrittlement problem presently encountered when tempering or isothermally transforming at temperatures above 250°C. This could also extend the operating range of 52100 steel bearings.

E. TENSILE TEST RESULTS

Tensile tests were conducted in order to better understand the mechanical property differences between the rolled and standard materials after isothermal transformation. The 650°C rolled material was selected for comparison to the standard 52100 steel. Table 5 contains the results of these tests.

After the 250°C heat treatment, both materials tested failed prior to yield. The 650°C material failed at a very low tensile stress, 935 MPa. This early failure, along with the low fracture toughness attained using this heat treatment, is difficult to explain. The rolled materials isothermally transformed at 250°C were found to have retained austenite as indicated in Table 4. Kar found [Ref. 7]

evidence to indicate that retained austenite improved the fracture toughness of 52100 steel. However, Hertzberg points out in Ref. 19 that retained austenite in high carbon steel, "can damage overall material response when it undergoes an ill-timed stress induced transformation to untempered martensite." This substantiates the belief that unstable retained austenite is responsible for the reduced fracture resistance in the rolled material.

The tensile tests conducted after the 300-IT heat treatment showed the rolled material and standard material to be compared in yield stress and ultimate tensile stress. The rolled material, however, displayed a greater ductility with 8.7 percent elongation, as compared to the standard material which had 5.4 percent elongation.

The reduction in area is also greater for the material previously rolled at 650°C, 25.3 percent versus 17.1 percent for the standard material. The mechanical properties for this material, rolled and given the isothermal transformation, are, then, impressive. The strength - toughness - ductility combination is like that of such low carbon steels as 300-M, a high strength alloy steel noted for its strength and toughness.

IV. CONCLUSIONS

Based on the experimental observations and results, the following conclusions are made:

1. The Sherby process does achieve a fine ferritic structure with small, iniformly dispersed carbides in AISI 52100 steel. The degree of refinement is better using a 650 C rolling temperature as opposed to a 550 C rolling temperature.

2. The refined carbide size and uniform distribution persists through subsequent heat treatment processes.

3. The smaller carbide size results in improved fracture toughness in the heat treated 52100 steel.

4. Increased dissolution of carbides at the 850 C austenitized and then quenched and tempered material resulted in higher hardness.

5. AISI 52100 steel rolled by the Sherby method exhibits higher ductility at room temperature with no loss of strength after isothermal transformation at 300 C.

6. Isothermal transformation after austenitization results in lower hardness than standard quench and temper treatments.

7. The effect of isothermal transformation on the toughness of the rolled and standard AISI 52100 steel varies with holding temperature. Also, the roll austenite plays in the reduced fracture toughness of the rolled material cannot be unequivocally stated as deleterious, but appears to be so.

Further study should place emphasis on this method of heat treatment, examining the effect of deep freezing after isothermal transformation to determine the roll austenite plays in the toughness of the rolled material, and investigating the toughness-hardness combinations obtained using holding temperatures between 250°C and 300°C.

APPENDIX A

CORRELATION BETWEEN APPARENT AND PLANE STRAIN FRACTURE TOUGHNESS

Heald, Spinks, and Worthington [Ref. 21] derived a model to correlate apparent fracture toughness to plane strain fracture toughness as a function of notch root radius (of a machined notch) and crack length c. Using linearly elastic fracture mechanics theory for propagation from a semi-elliptical notch, the apparent fracture toughness was defined as:

$$K_Q(\rho) = \frac{\pi c^{\frac{1}{2}} \sigma_u}{(1+(\rho/c))^{\frac{1}{2}}} \times \frac{2}{\pi} \cos^{-1}\left(\exp - \left(\frac{\pi K_{IC}^2}{8\sigma_u^2 c}\right)\right) + (\rho/c)^{\frac{1}{2}}$$

where

K_Q = Apparent Fracture Toughness

K_{IC} = Plane Strain Fracture Toughness

ρ = Root Radius of notch

σ_u = Ultimate tensile strength

c = Total crack length

Separating variables, and usint a Taylor series explanation, it can be shown that

$$K_{IC} = K_Q (1 + (\rho/c)^{\frac{1}{2}}) - \rho\pi\sigma_u$$

As the root radius approaches zero, K_Q approaches K_{IC}.

Applying this equation to data obtained for the standard 52100 in this research, gives results generally lower than

others report for this material. Since applying this equation would not alter the relative values of toughness, K_Q has been used for comparison throughout.

TABLE 1

ALLOY COMPOSITIONS

	C	Si	Cr	Mn	P	Al	Cu	Mo	Ni	Fe
1.	1.02	0.27	1.35	0.35	4.007	0.03	0.11	0.06	0.18	BALANCE
2.	1.06	0.27	1.37	0.36	0.008	0.03	0.03	0.06	0.07	BALANCE

Note: (1) Vasco Pacific Steel Company Material

(2) Carpenter Steel Company

TABLE 2
HEAT TREATMENTS

Symbol	Treatment
1. 775-ST	Austenitization at 775 C 20 min, warm oil quench to 50 C, standard temper
2. 850-ST	Austenitization at 850 C for 20 min, warm oil quench to 50 C, standard temper
3. 250-IT	Austentization at 850 C for 20 min, isothermal tranformation at 250 C for 1 hr., warm oil quench to 50 C, air cool.
4. 300-IT	Austenitization at 850 C for 20 min., isothermal transformation at 250 C for 1 hr., warm oil quench to 50 C, air cool

TABLE 3

RESULTS OF FRACTURE TOUGHNESS TESTING

FOR AISI 52100 STEEL IN HARDENED CONDITION

Material	Treatment	Apparent Fracture Toughness ($MPa\text{-}m^{\frac{1}{2}}$)	Apparent Fracture Toughness ($ksi\text{-}in^{\frac{1}{2}}$)	Hardness (R_C)
1. 650 C Rolled	775-ST	37.5	34.1	60.0
2. 550 C Rolled	775-ST	36.2	32.9	59.5
3. Standard	775-ST	34.9	31.8	59.6
4. 650 C Rolled	850-ST	28.1	25.6	62.8
5. 550 C Rolled	850-ST	25.6	23.3	63.5
6. Standard	850-ST	22.9	20.8	61.7

TABLE 4

RESULTS OF FRACTURE TOUGHNESS TESTS FOR 52100 ISOTHERMALLY TRANSFORMED

Material	Treatment	Apparent Fracture Toughness (Ksi-in$^{\frac{1}{2}}$)	(MPa-m$^{\frac{1}{2}}$)	Pct Retrieved austenite (unstressed)	Hardness (R_C)
1. 650°C Rolled	250	28.4	31.2	10.2	59
2. 550°C Rolled	250	28.7	31.5	16.2	59
3. Standard (Double Melted)	250	40.5	44.5	< 5.0	58.5
4. 650°C Rolled	300	79.0	86.8	< 5.0	50.0
5. 650°C Rolled	300	50.0	55.5	< 5.0	53.3
6. Standard (Double Melted)	300	28.6	31.4	< 5.0	53.6

TABLE 5

TENSILE TEST RESULTS FOR 52100 STEEL

Material	Treatment	Yield Stress (Ksi)	(MPa)	Ultimate Tensil Strength (Ksi)	(MPa)	Pct Elongation	Fracture Surface Reduction
650°C Rolled	250-IT	Broke Before Yield		135.7	935.6	-	-
Standard 5211	250-IT	Broke Before Yield		213.3	1470.6	-	-
650°C	300-IT	256	1765.0	297.2	2049.1	8.7	25.3%
Standard 52100	300-IT	259	1785.7	295.1	2034.6	5.4	17.1%

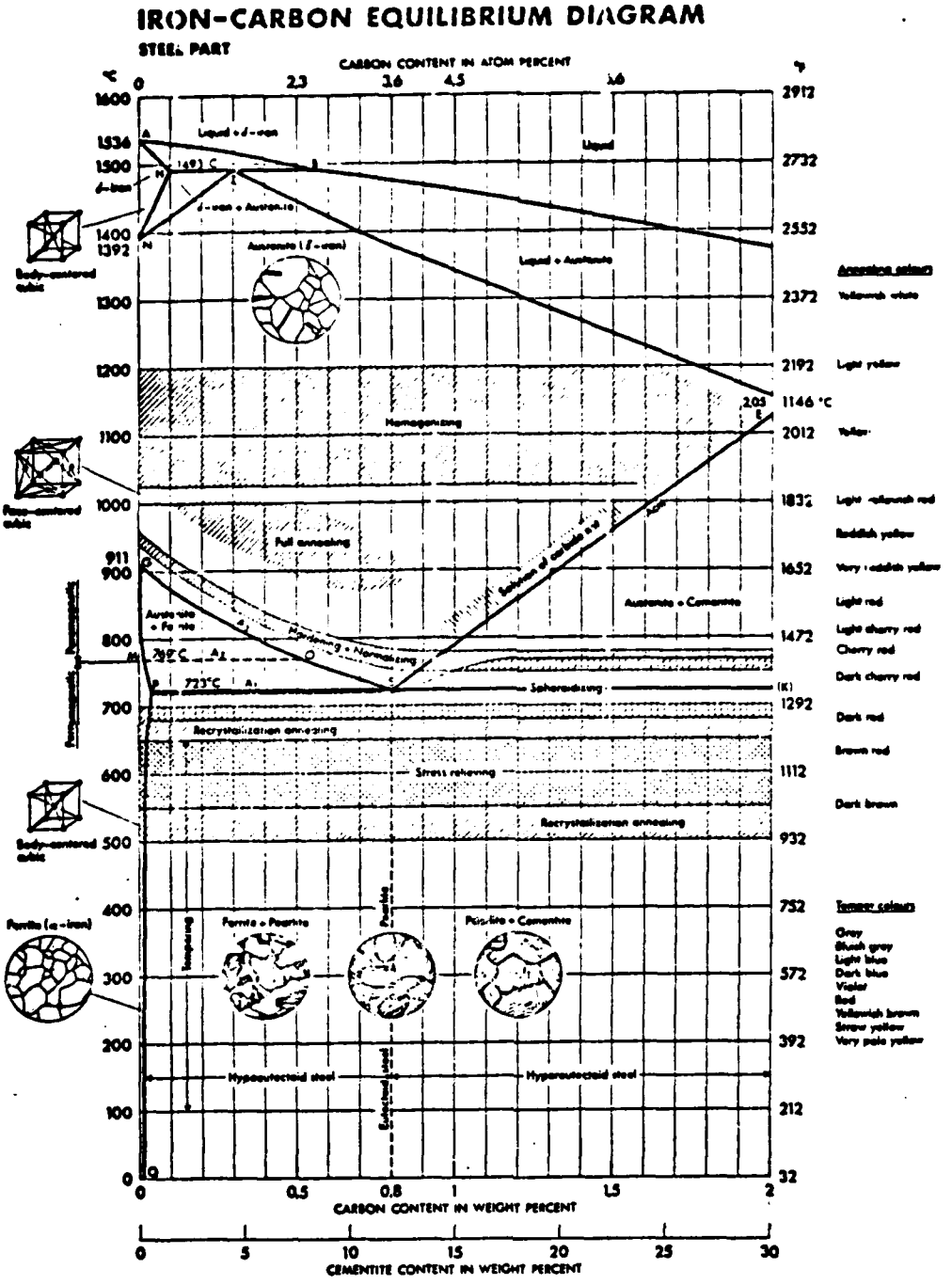

Figure 1. Fe-C Equilibrium Phase Diagram. Note the spheroidizing region around the eutectoid temperature, 723 C.

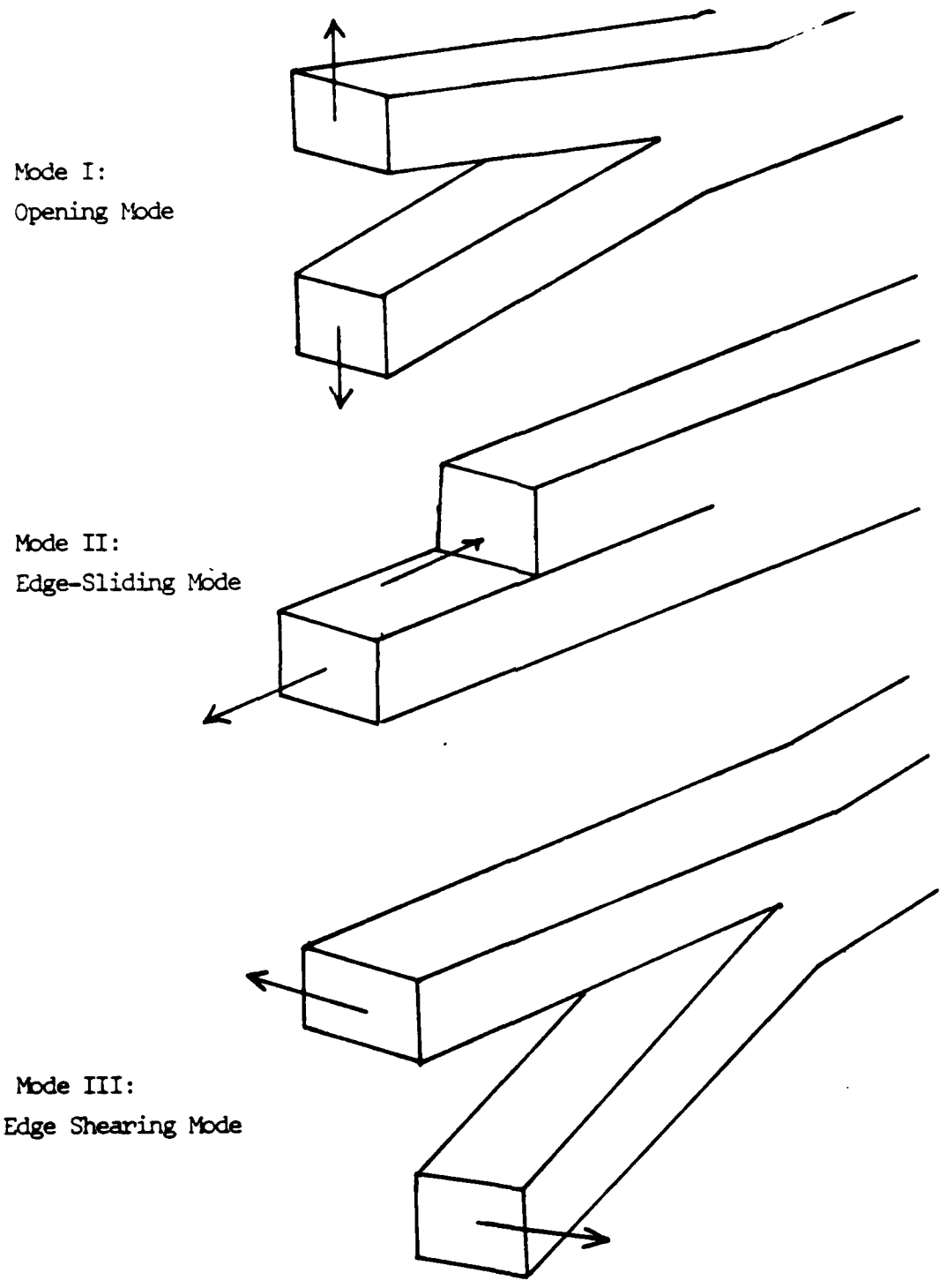

Figure 2. Diagram Of Stress Fields Near A Crack Tip. These drawings depict the three basic modes of crack propagation.

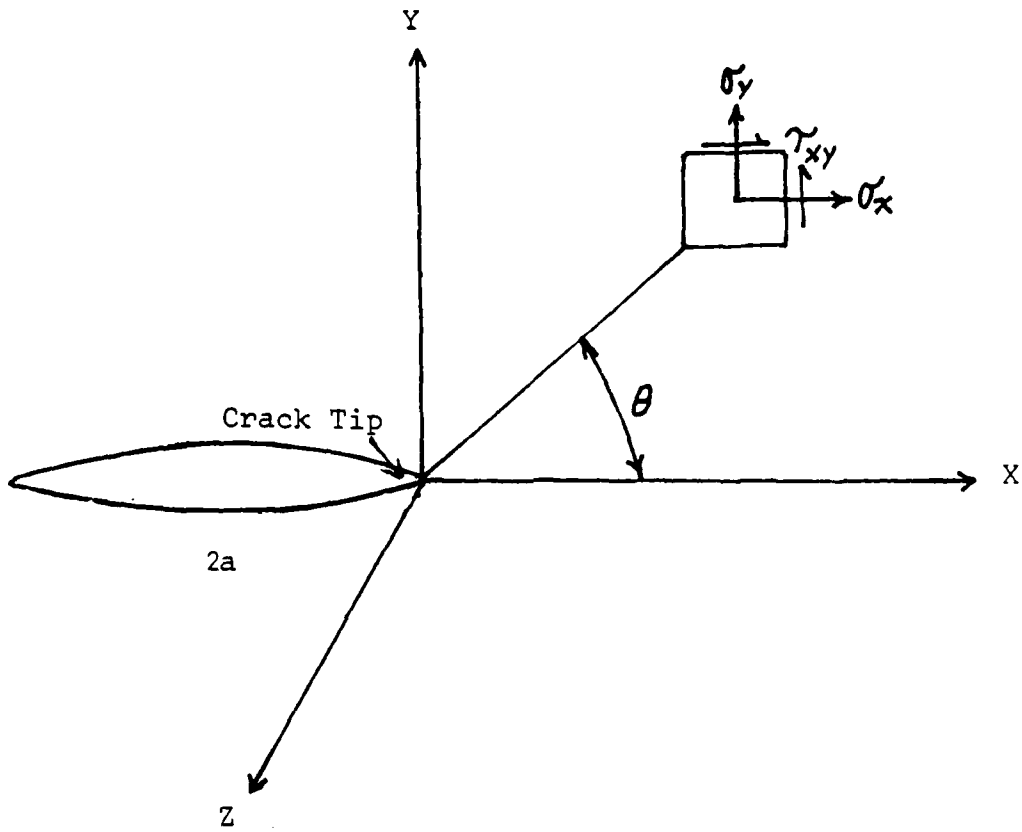

Figure 3. Diagram Of Stress Distribution Around A Crack Tip.

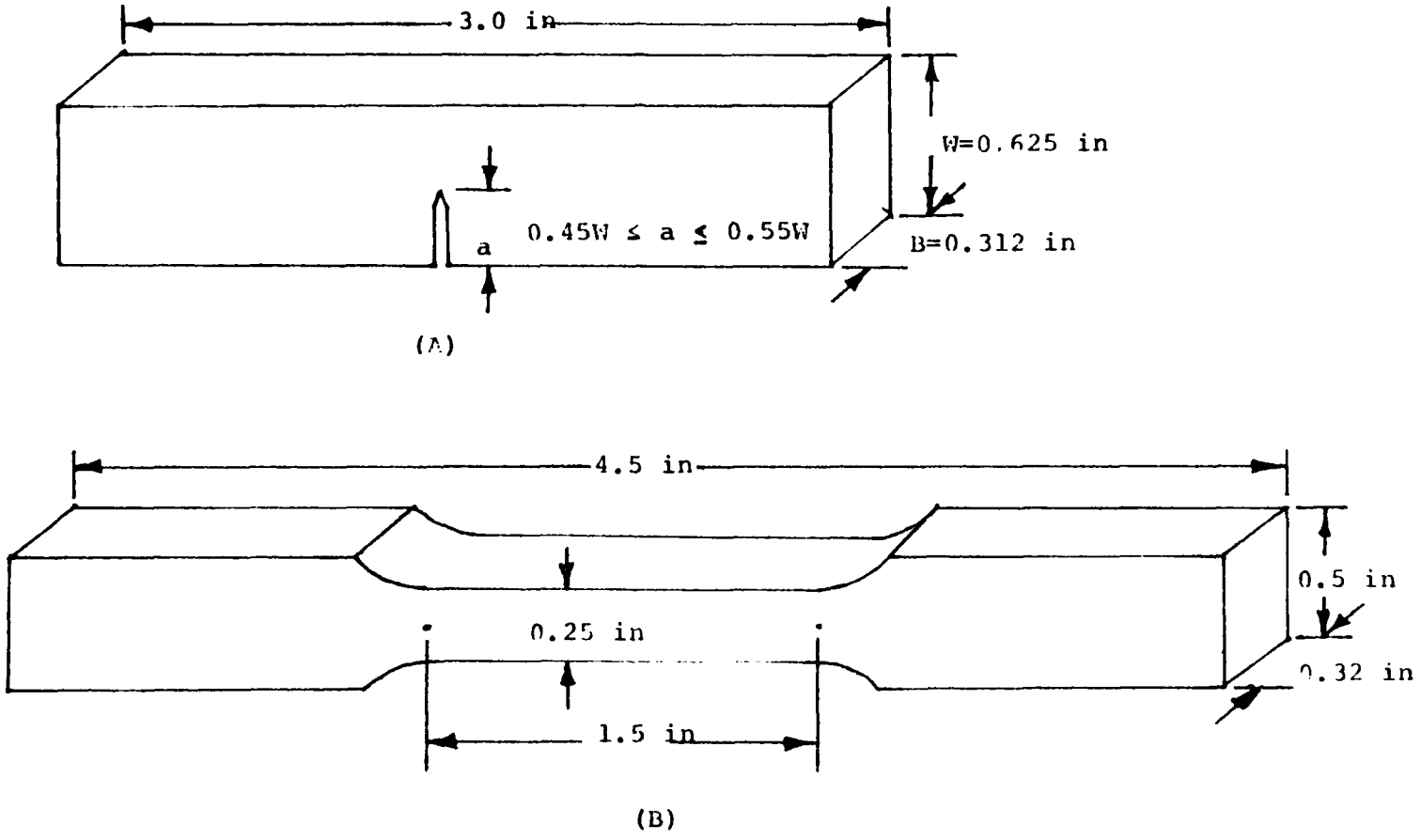

Figure 4. Test Specimen Specifications. These drawings depict the dimensions of the 52100 steel samples used in fraction toughness (A) and Tensile Tests (B).

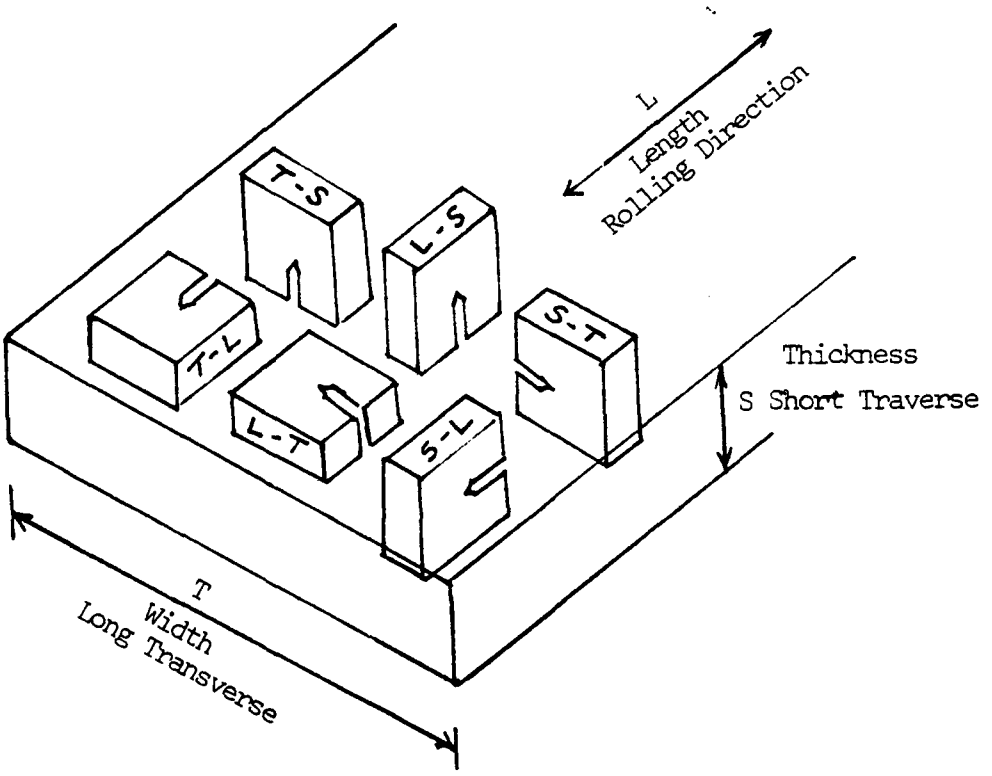

Figure 5. Rolling Direction Orientation. This drawing depicts the orientation terminology of a notch with respect to the rolling (longitudinal) direction.

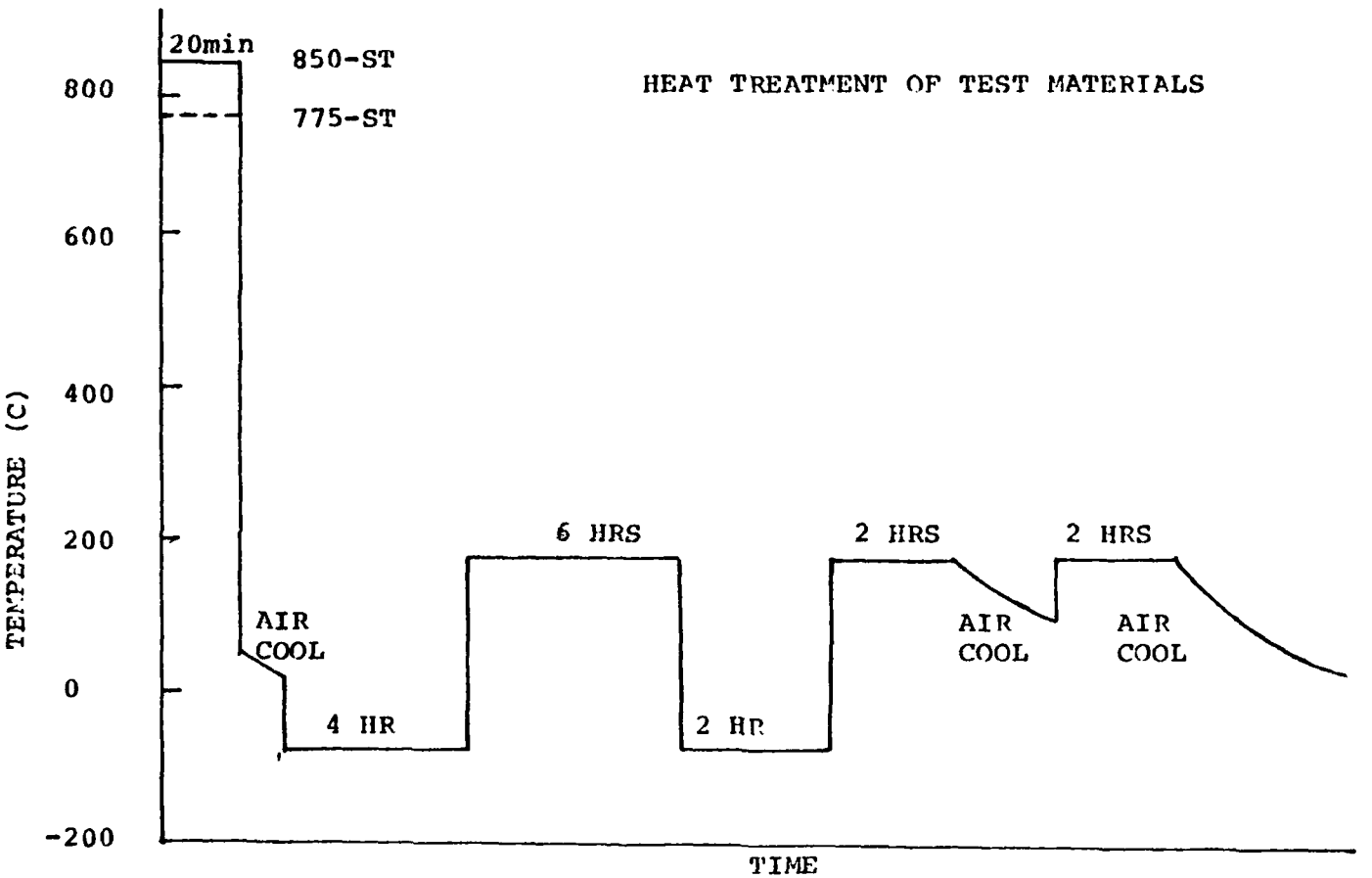

Figure 6. Standard Temper Heat Treatments. This schematic represents the treatment process for the 775-ST and 850 hardening treatments.

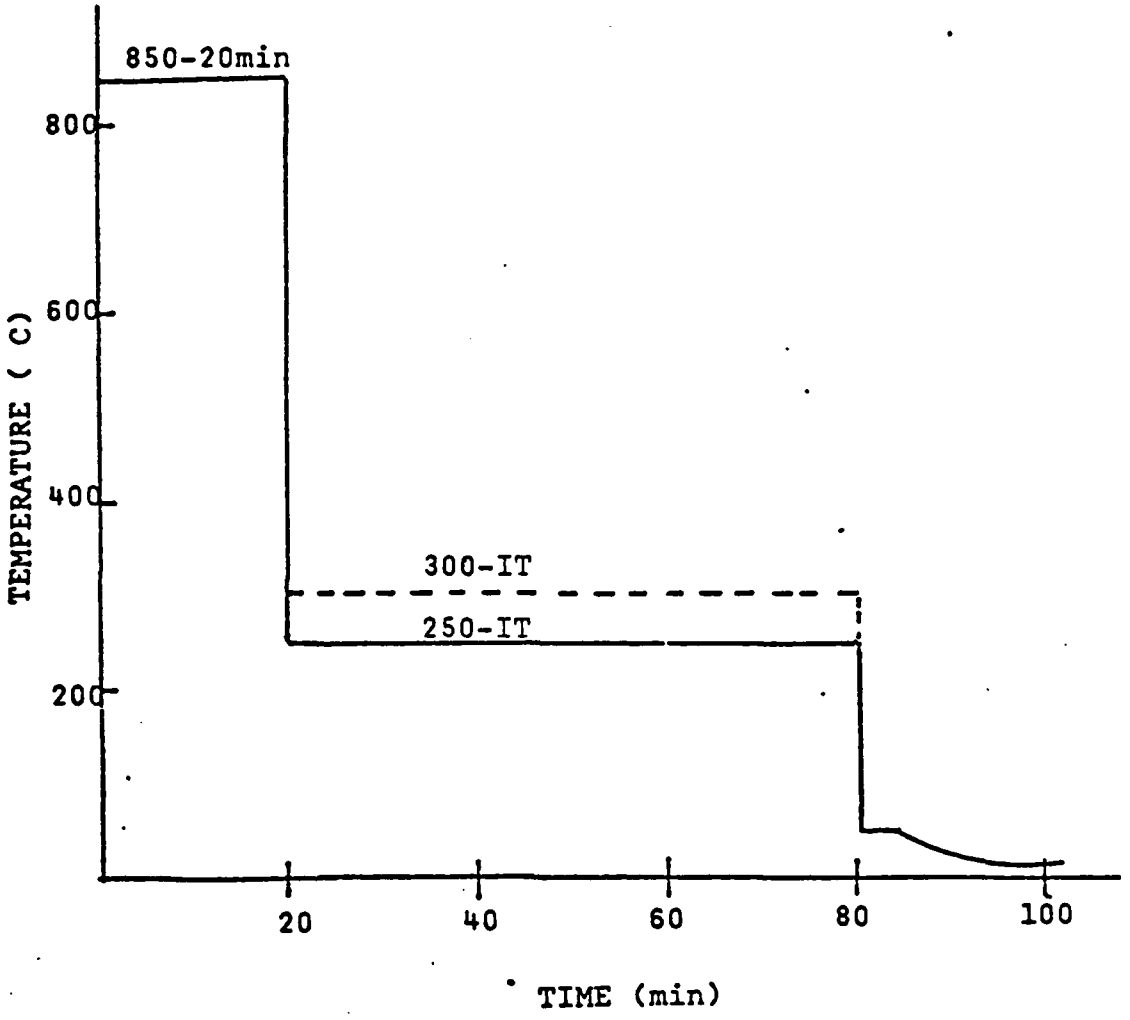

Figure 7. Isothermal Transformation Heat Treatments. This drawing schematically represents the 250-IT and 300-IT Hardening treatments.

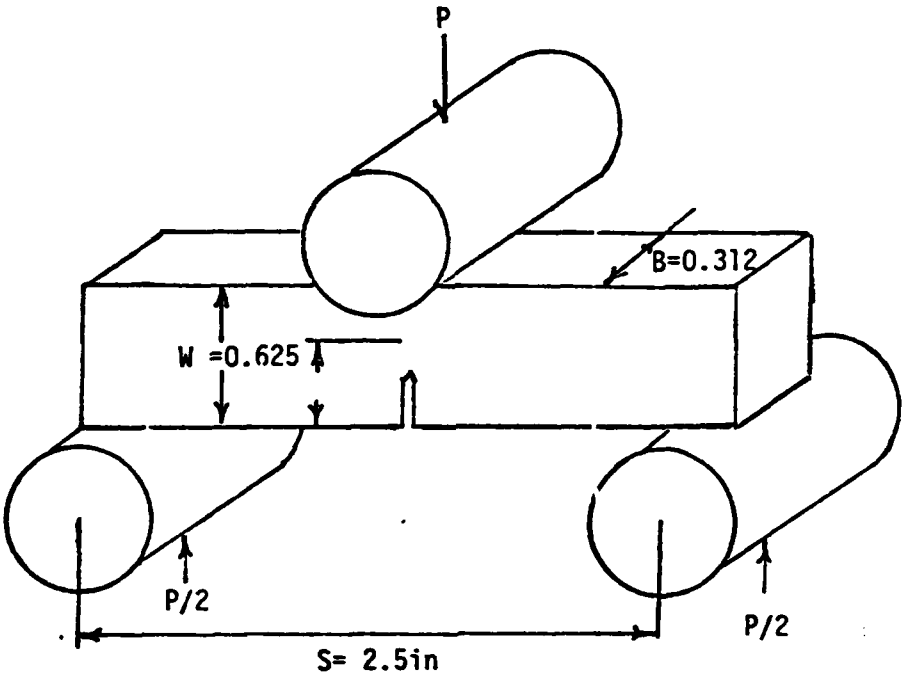

Figure 8. Plane Strain Toughness Test Specimen Loading. This drawing shows the loading configuration of the three point bend test specimen as dictated by ASTM Standard E399-78.

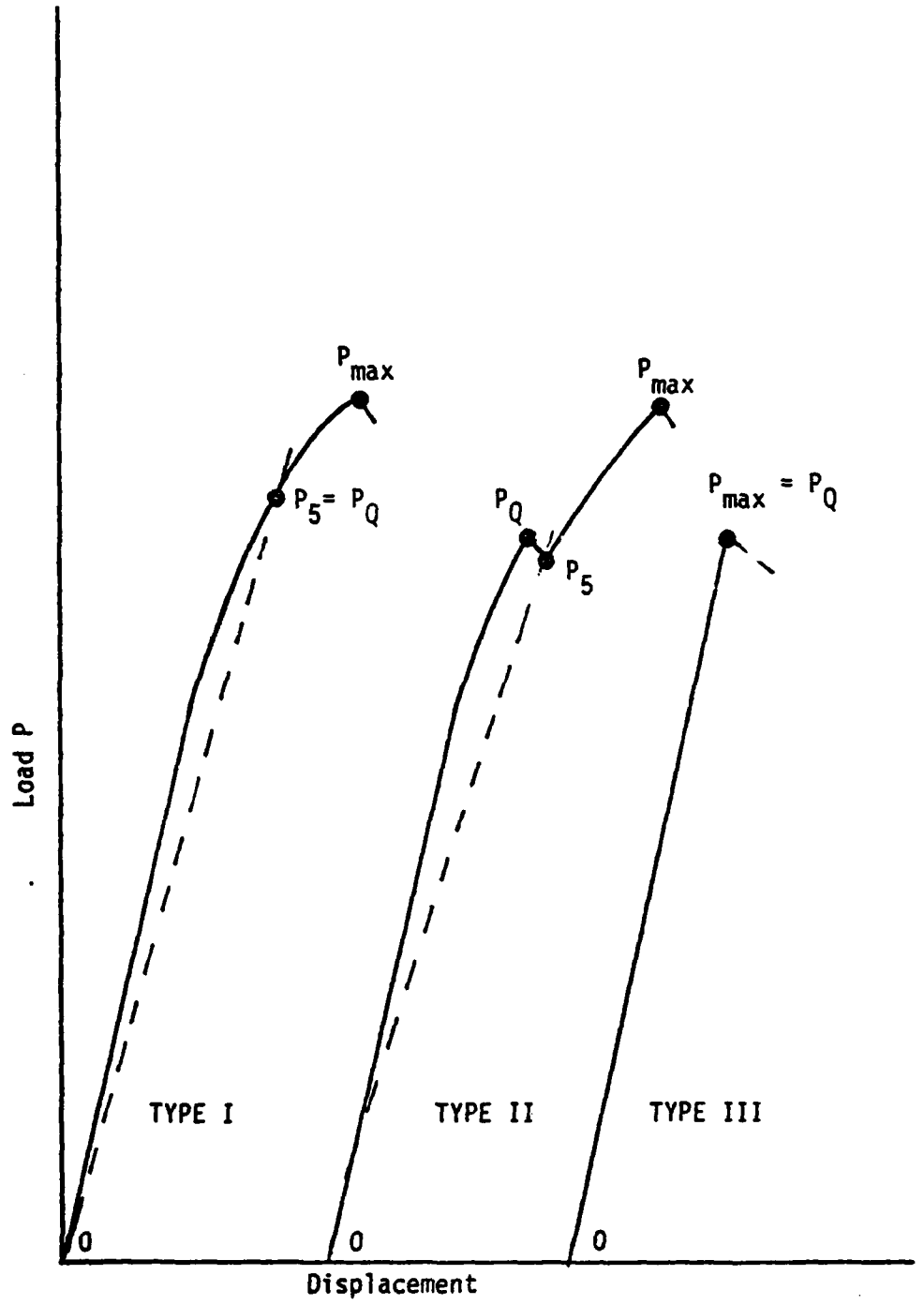

Figure 9. Load Versus Crack Opening Displacement. This graph indicates the method used in determining the fracture load used in calculating apparent fracutre toughness as dictated by ASTM Standard E399-78.

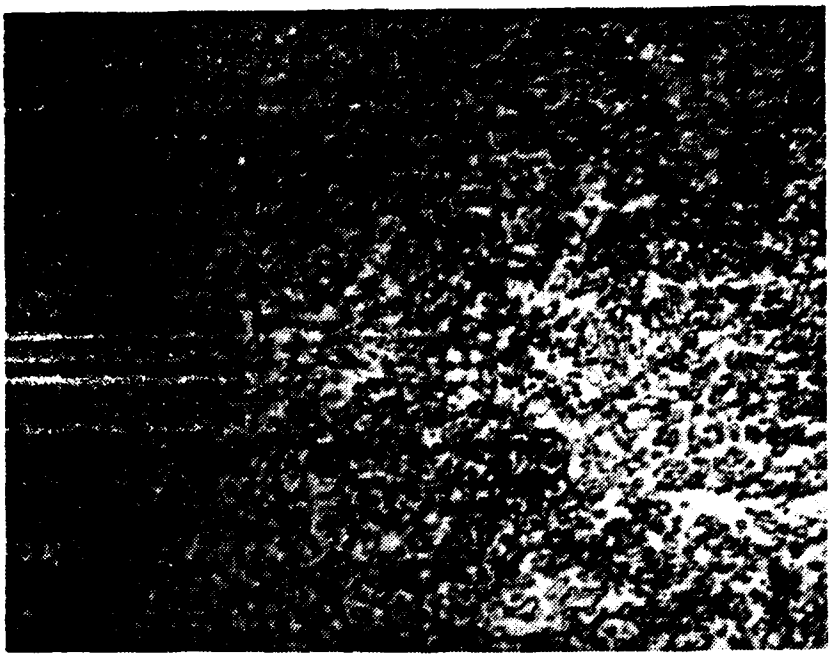

Figure 10. Micrograph Of Standard 52100 Steel Etched In 2% Nital Solution. Microstructure consists of coarse carbides in a ferrite matrix.

Figure 11. Micrograph of 650 C Rolled 52100 Etched In 2% Nital Solution. This microstructure consists of small carbides in a fine ferrite matrix. 1000X

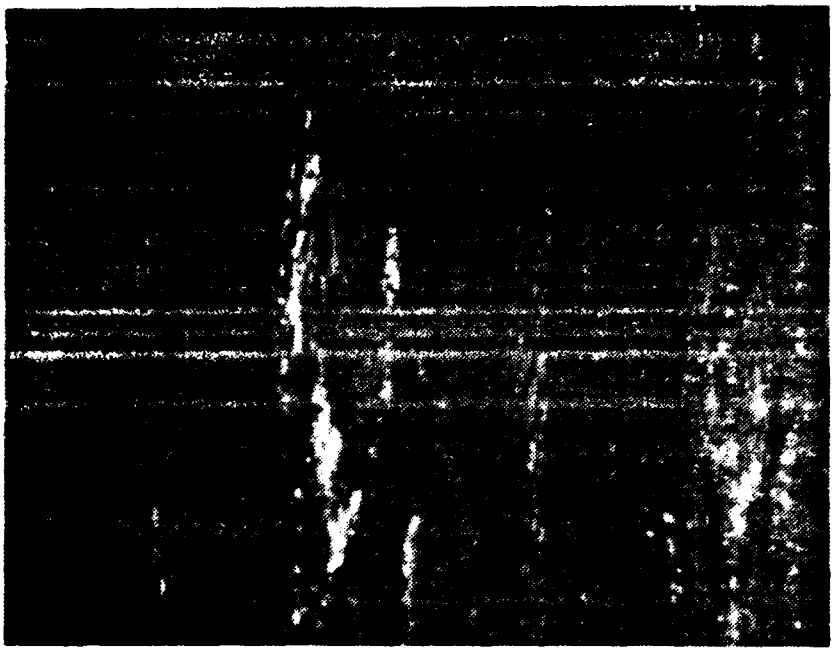

Figure 12. Micrograph Of 550 C Rolled 52100. Note the carbide size as compared to the 650 C rolled (Fig. 11). 1000X

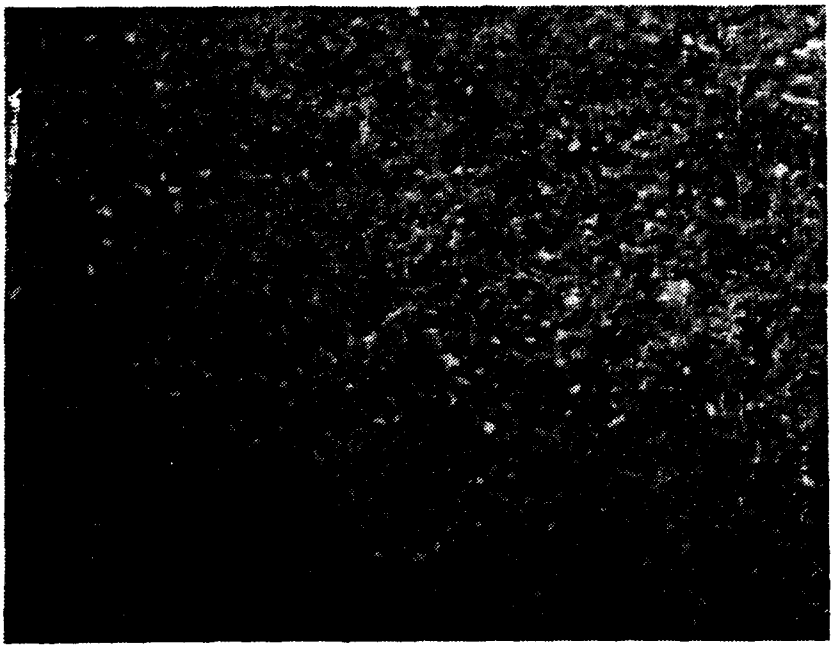

Figure 13. Micrograph Of Standard 52100 After Treatment 775-ST. Note the coarse carbides present after hardening. 1000X

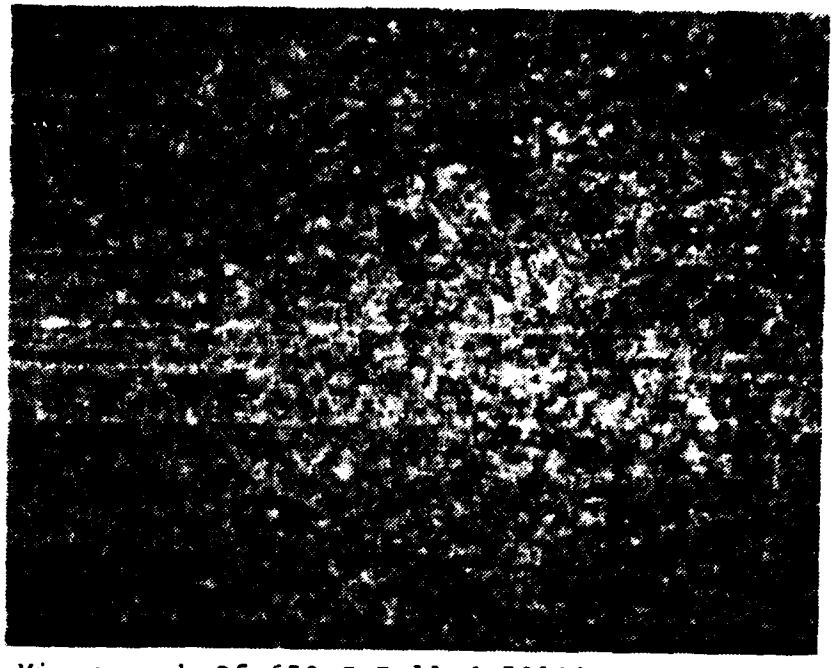

Figure 14. Micrograph Of 650 C Rolled 52100. The fine microstructure is a result of the rolling process. 1000X

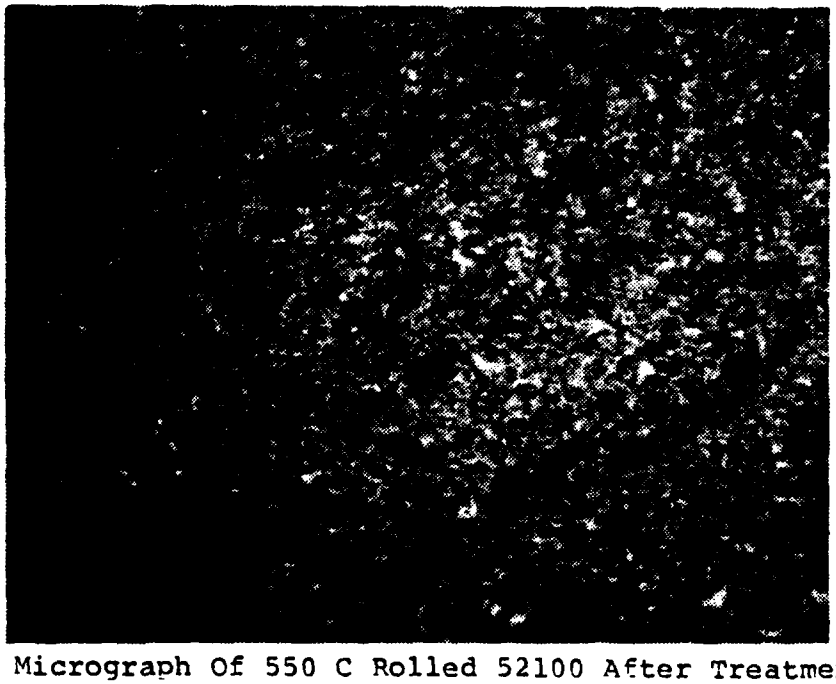

Figure 15. Micrograph Of 550 C Rolled 52100 After Treatment 775-ST. Microstructure consists of tempered martensite. 1000X

Figure 16. Micrograph Of Standard 52100 After Treatment 850-ST. Micrograph consists of tempered martensite with coarse carbides.

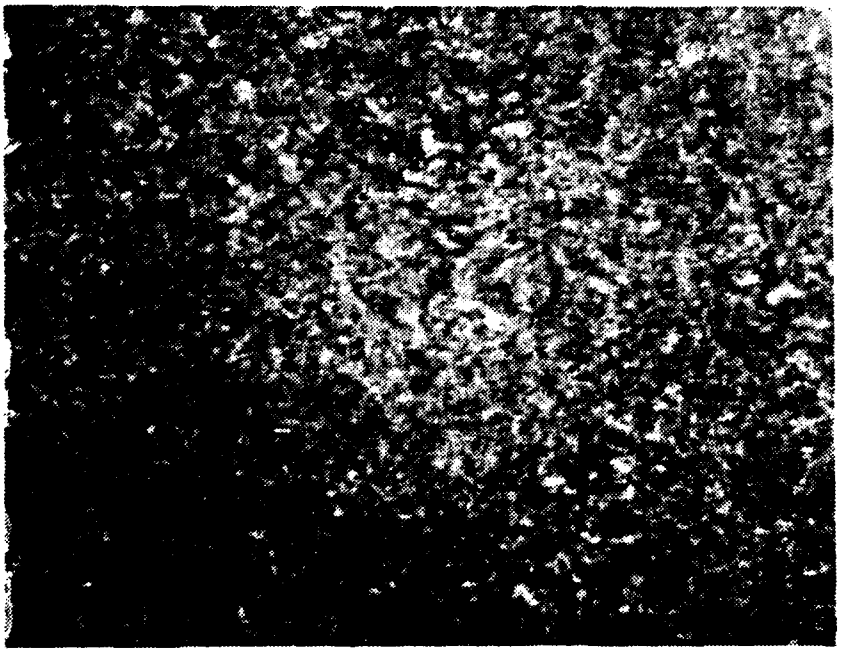

Figure 17. Micrograph Of 650 C Rolled 52100 After Treatment 850-ST. Micrograph consists of tempered martensite with very fine undissolved carbides. 1000X

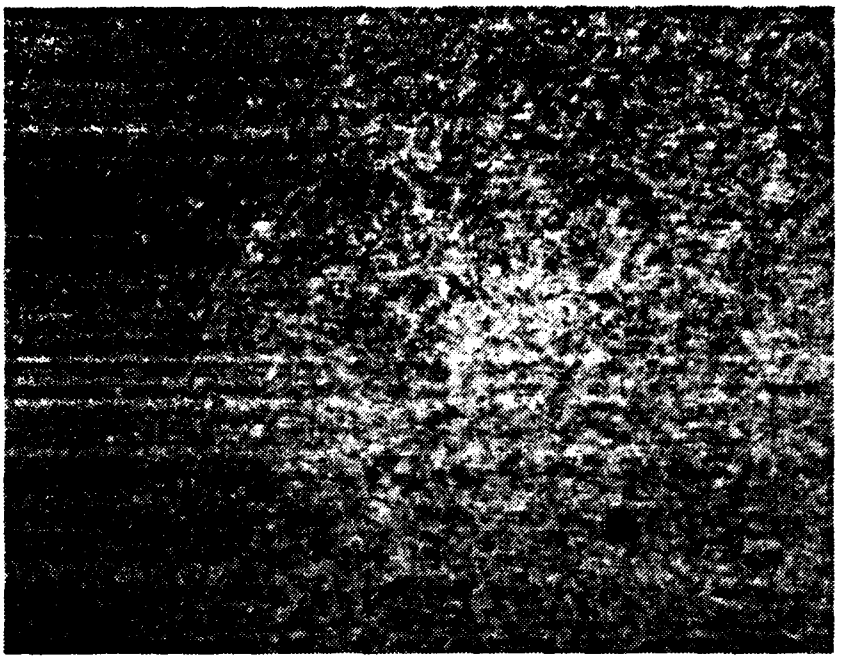

Figure 18. Micrograph Of 550 C Rolled Material After Treatment 850-ST. Micrograph consists of tempered martensite with undissolved carbides present. 1000X

Figure 19. Micrograph Of Standard 52100 After Treatment 250-IT. Micrograph consists of undissolved carbides in a bainitic structure. 1000X

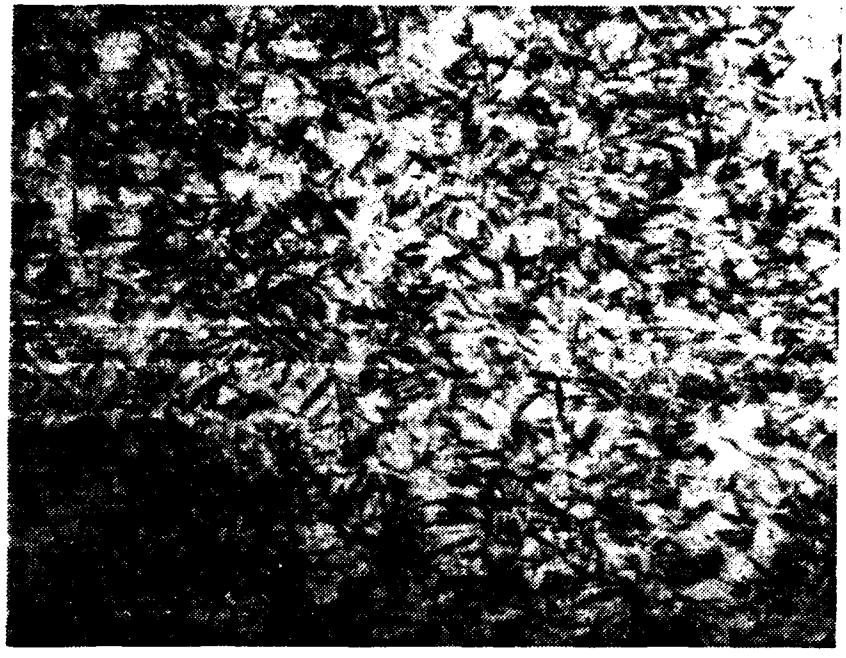

Figure 20. Micrograph Of 650 C Rolled Material After Treatment 250-IT. Microstructure consists of a combination of bainite and martensite. 1000X

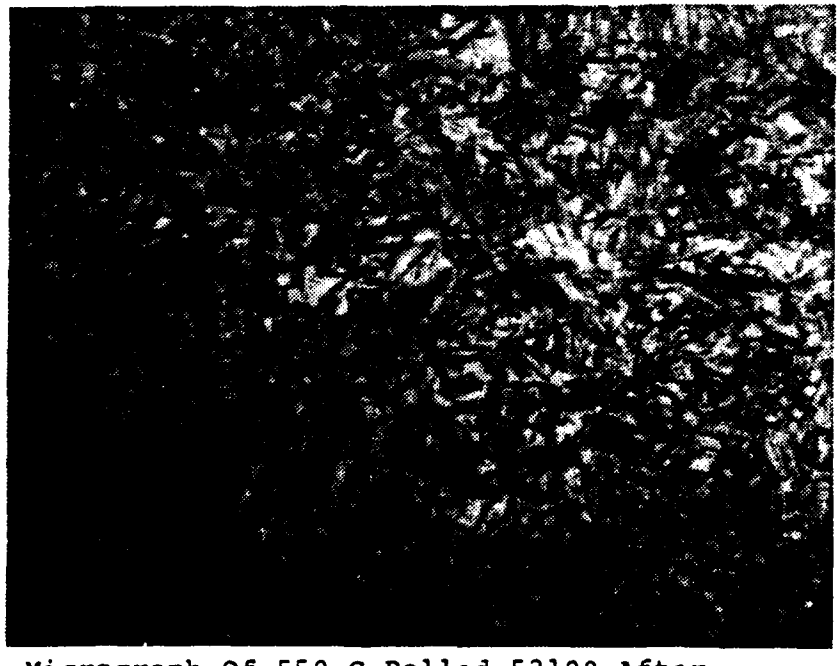

Figure 21. Micrograph Of 550 C Rolled 52100 After Treatment 250-IT. Microstructure consists of bainite and martensite. 1000X

Figure 22. Micrograph Of Standard 52100 After Treatment 300-IT. This is a primarily bainitic structure with undissolved carbides. 1000X

Figure 23. Micrograph Of 650 C Rolled 52100 After Treatment 300-IT. This structure is bainitic with no undissolved carbides in evidence. 1000X

Figure 24. Micrograph of 550 C Rolled 52100 After Treatment 300-IT. Note the apparent grain growth as compared to Fig. 21.

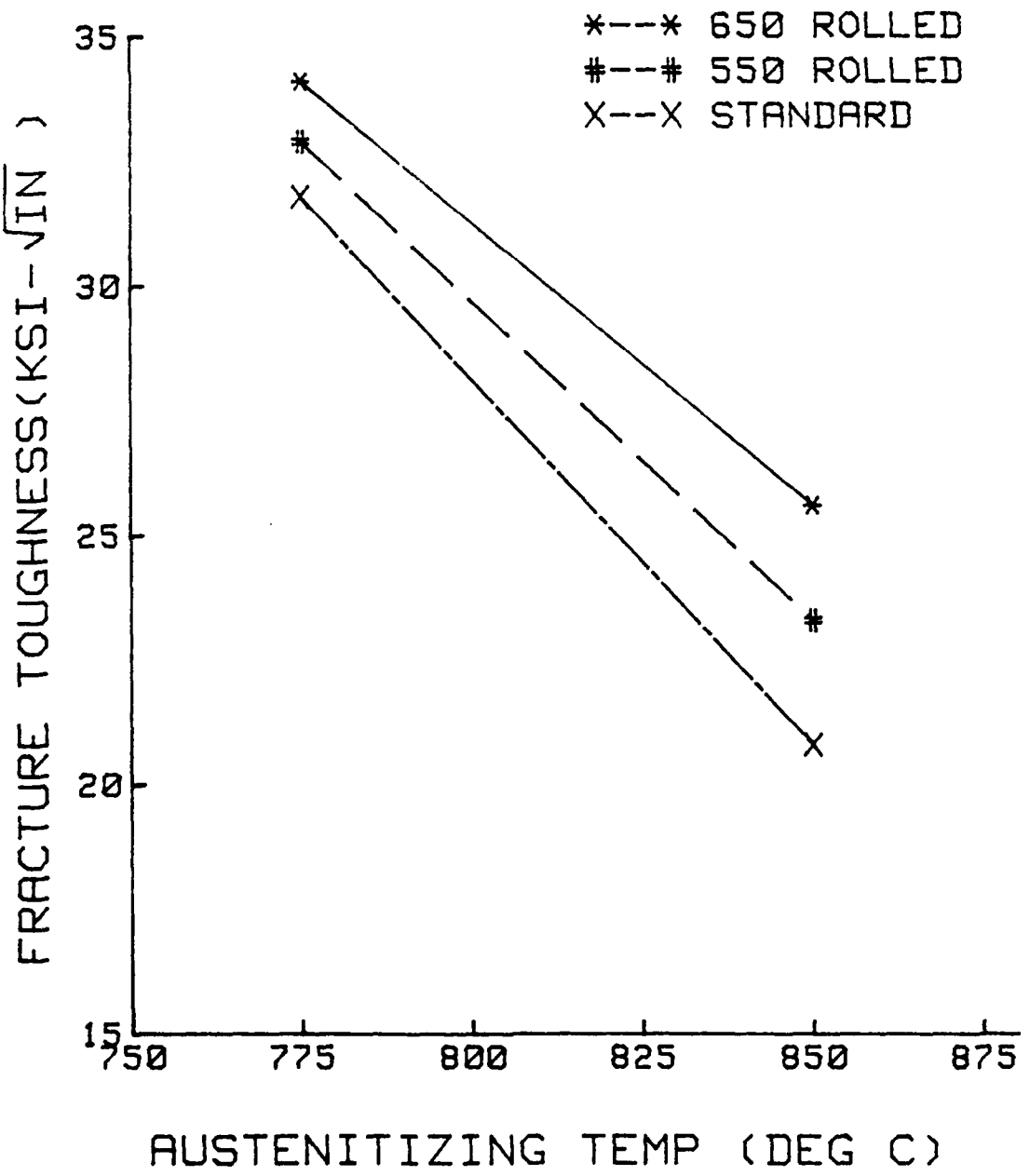

Figure 25. Fracture Toughness vs. Austenitizing Temperature For The Material Given Conventional Hardening Treatments.

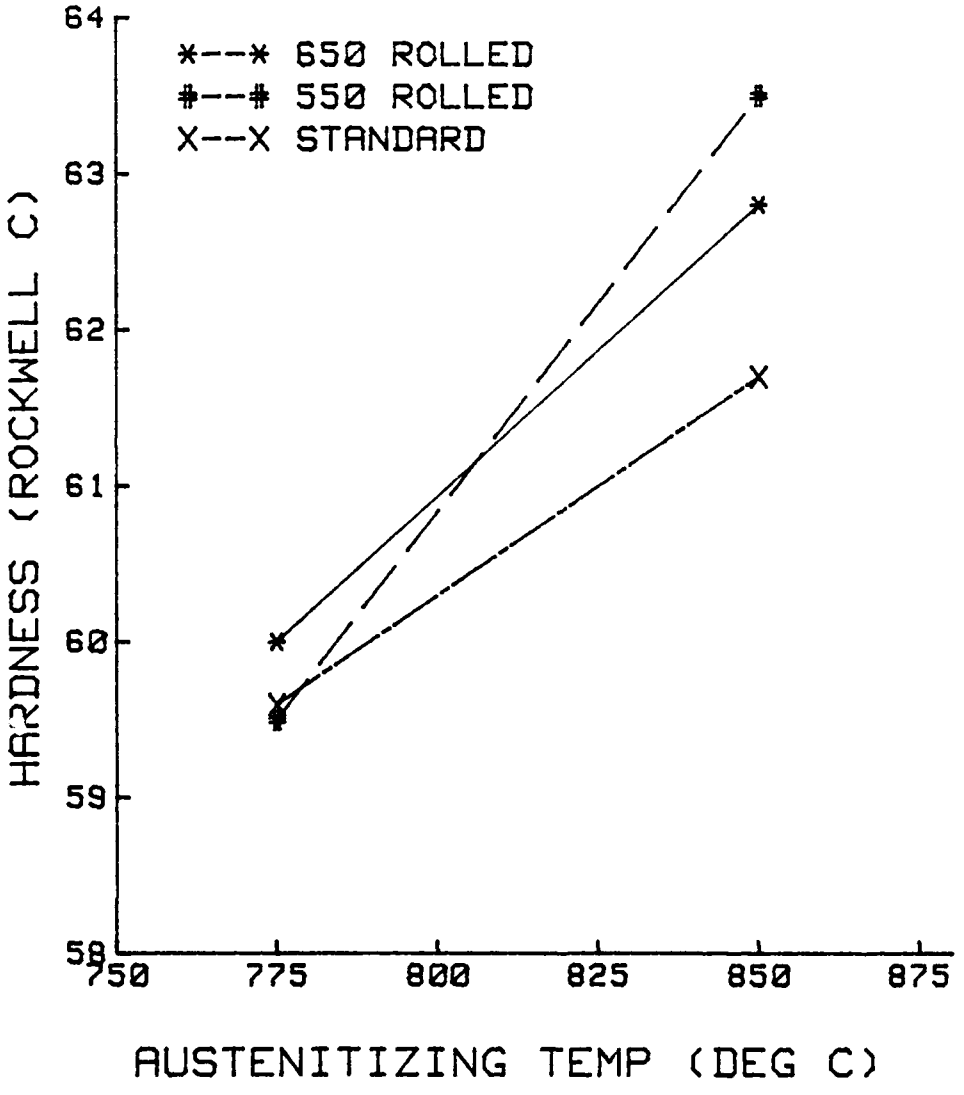

Figure 26. Hardness vs. Austenitizing Temperature For The Material Given Conventional Hardening Treatments.

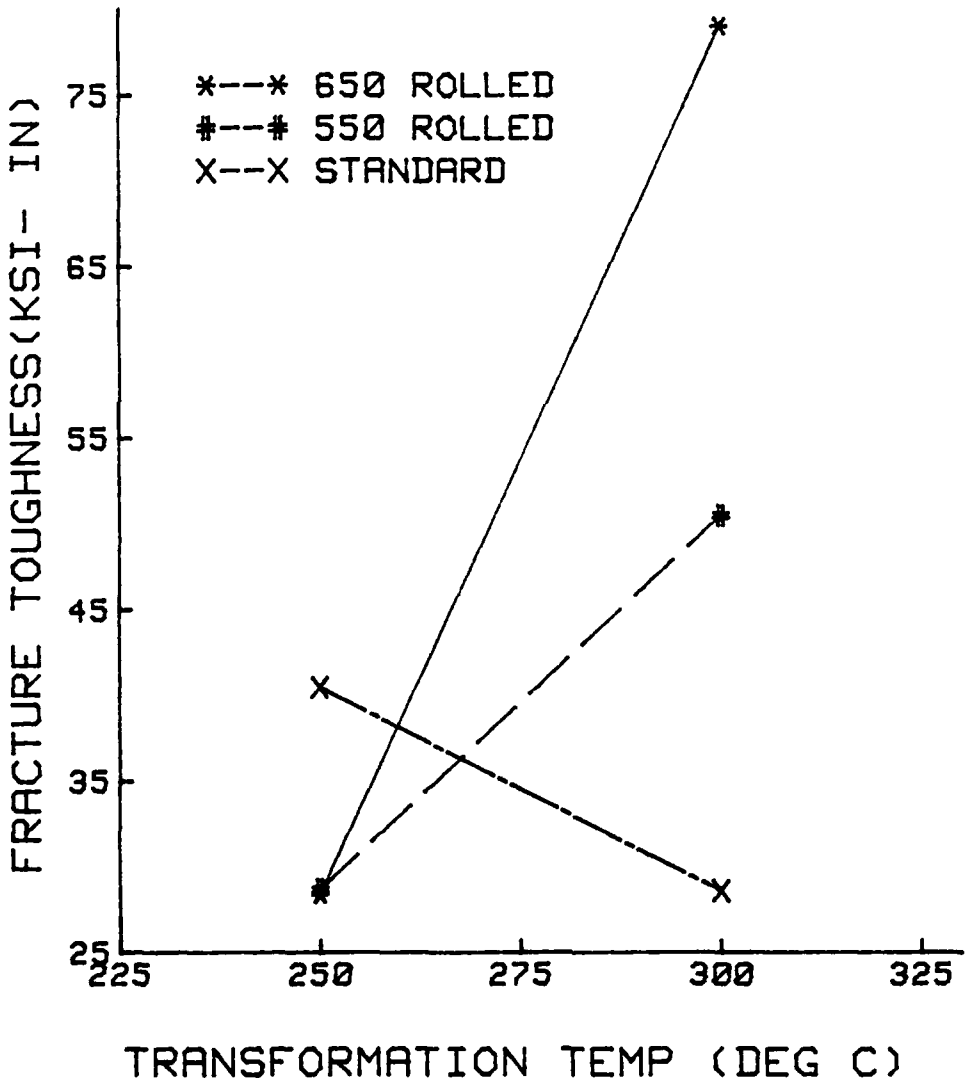

Figure 27. Fracture Toughness vs. Austenitizing Temperature For The Material Given The Isothermal Transformation Treatments.

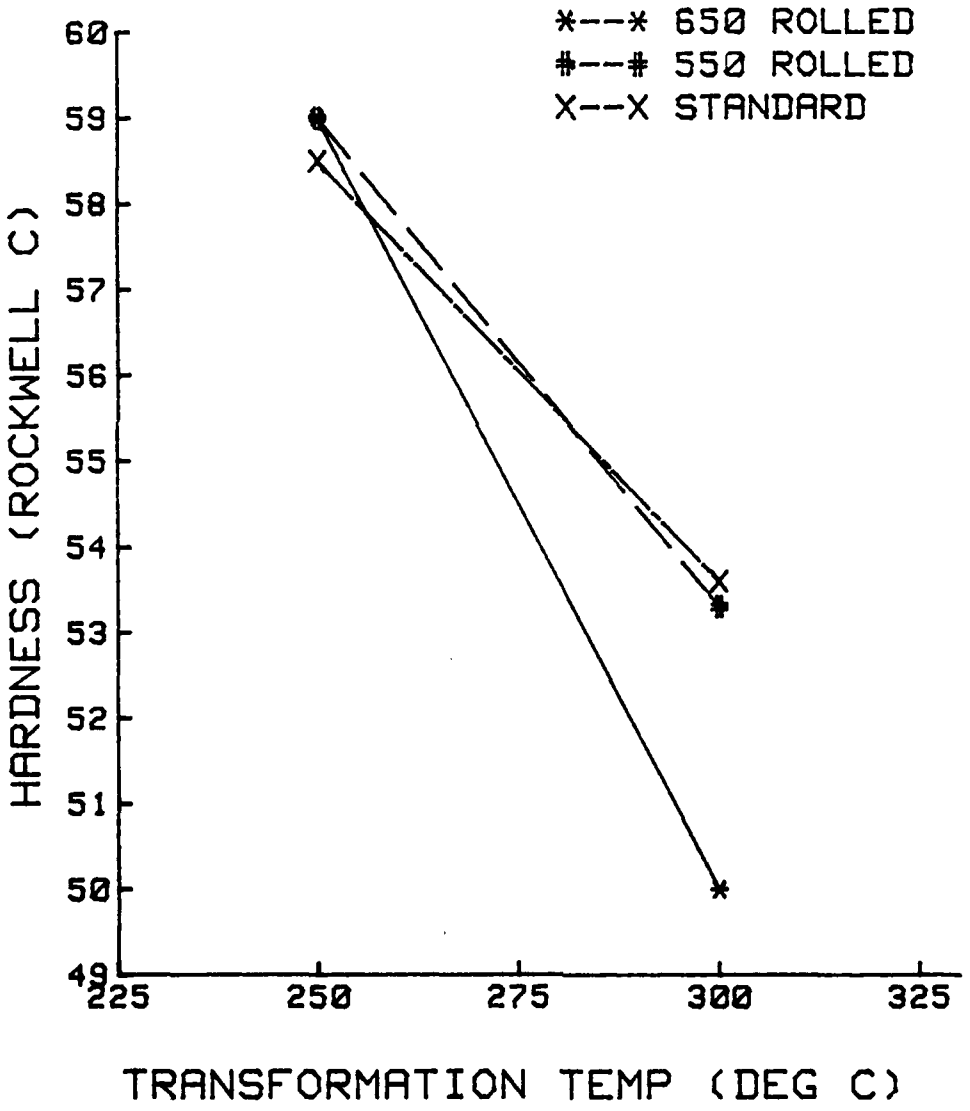

Figure 28. Hardness vs. Austenitizing Temperature For The Material Given Isothermal Transformation Treatments.

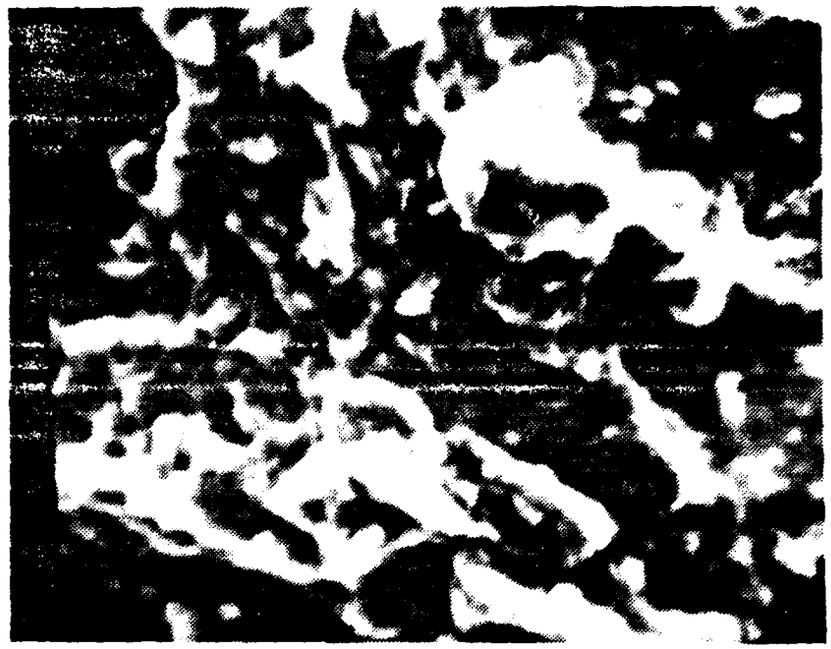

Figure 29. Fractograph Of Fracture Surface Of Standard 52100 Steel After Heat Treatment 775-ST. The surface indicates a primarily brittle fracture. 2000X

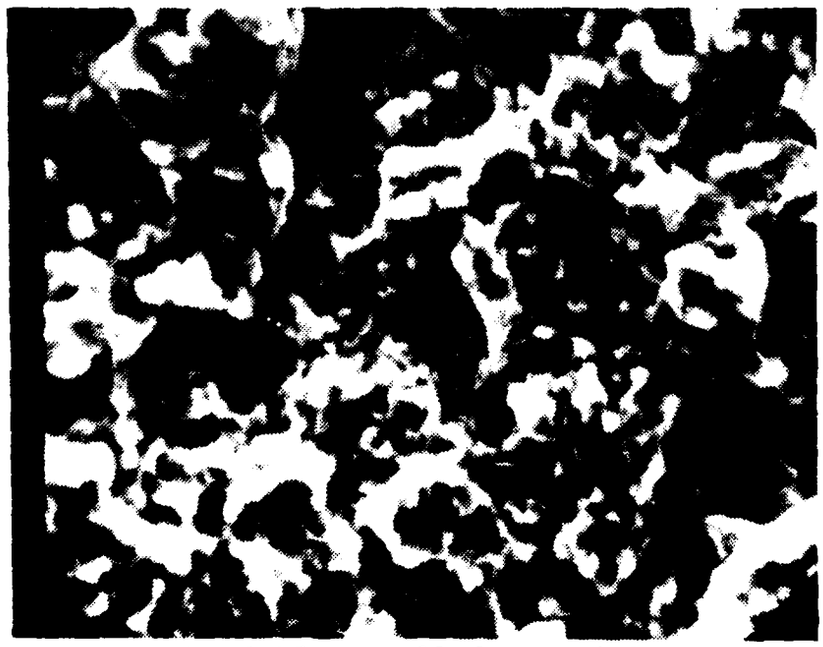

Figure 30. Fractograph Of 550 C Rolled Material Fracture Surface After Heat Treatment 775-ST. The surface indicates brittle fracture. 2000X

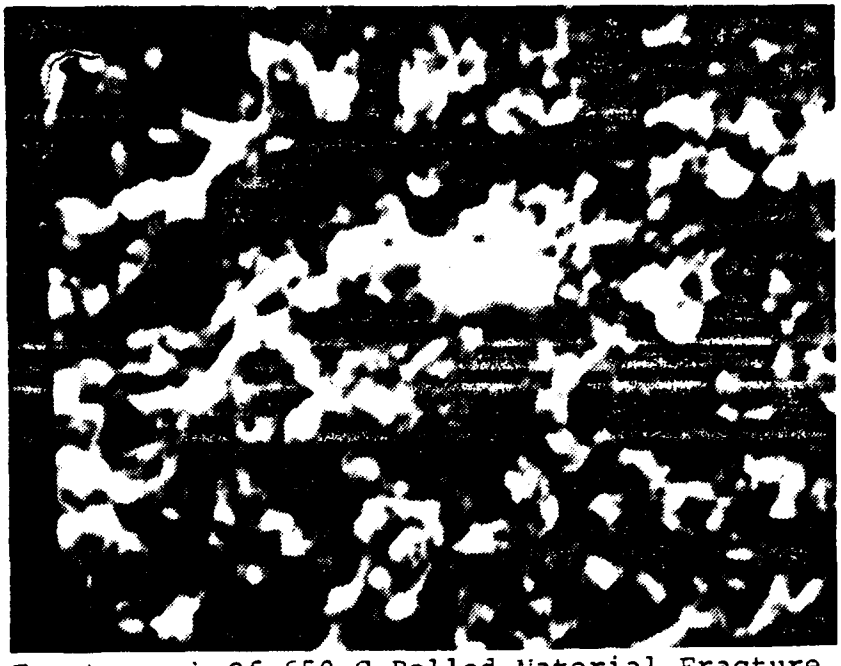

Figure 31. Fractograph Of 650 C Rolled Material Fracture Surface After Hardening Treatment 775-ST. Note the apparent decrease in size of cleavage facets as compared to Fig. 30. 2000X

Figure 32. Fractograph Of Standard 52100 Fracture Surface After Hardening Treatment 850-ST. The flat surfaces are clear evidence of brittle fracture. 2000X

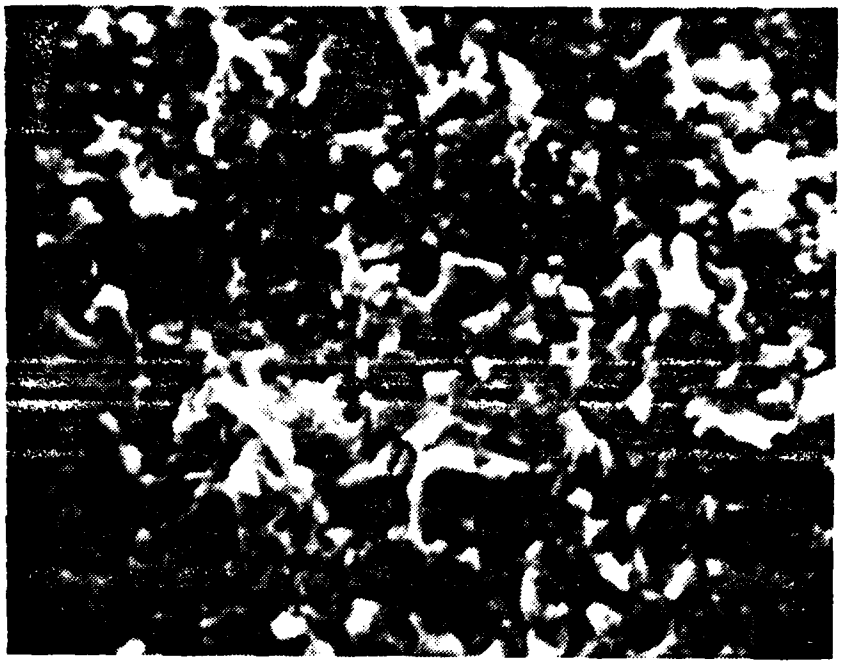

Figure 33. Fractograph Of 550 C Rolled 52100 Material After Hardening Treatment 850-ST. The grain refining effect of rolling is evident. This surface indicates a quasi-cleavage brittle fracture. 2000X

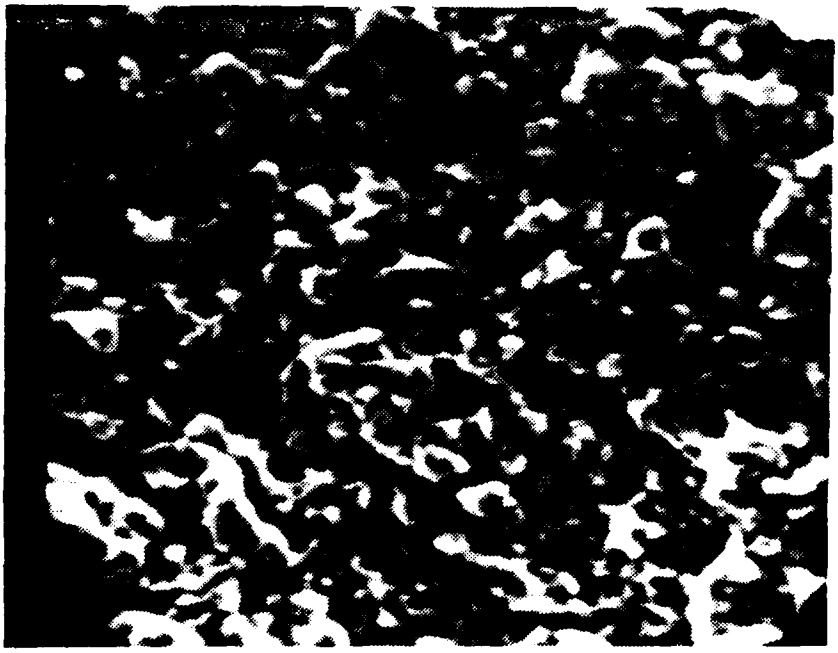

Figure 34. Fractograph of 650 C Rolled Material Fracture Surface After Hardening Treatment 850-ST. This indicates a quasi-cleavage form of failure. 2000X

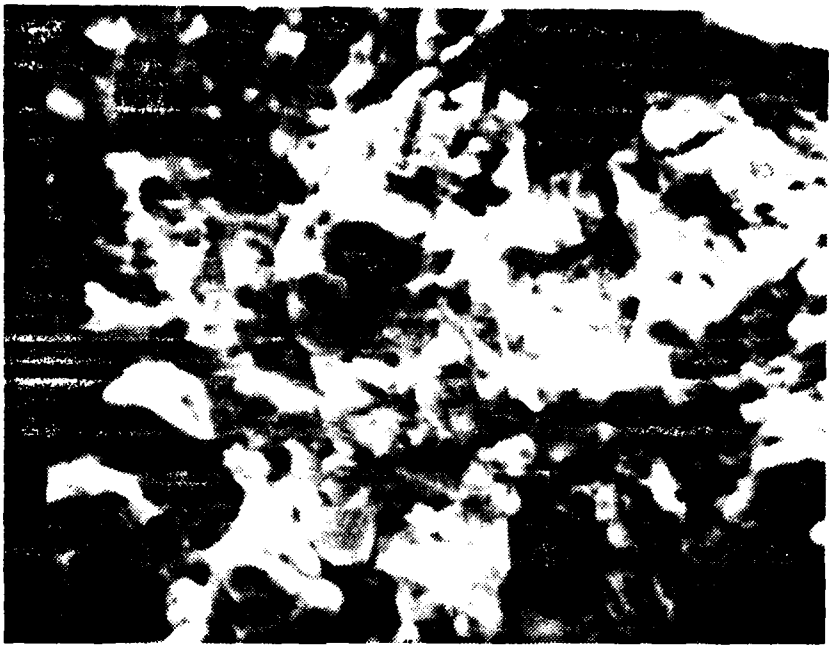

Figure 35. Fractograph Of Standard 52100 Material After Hardening Treatment 250-IT. Note the increased number of dimples as compared to this same material given the 850-ST treatment. 2000X

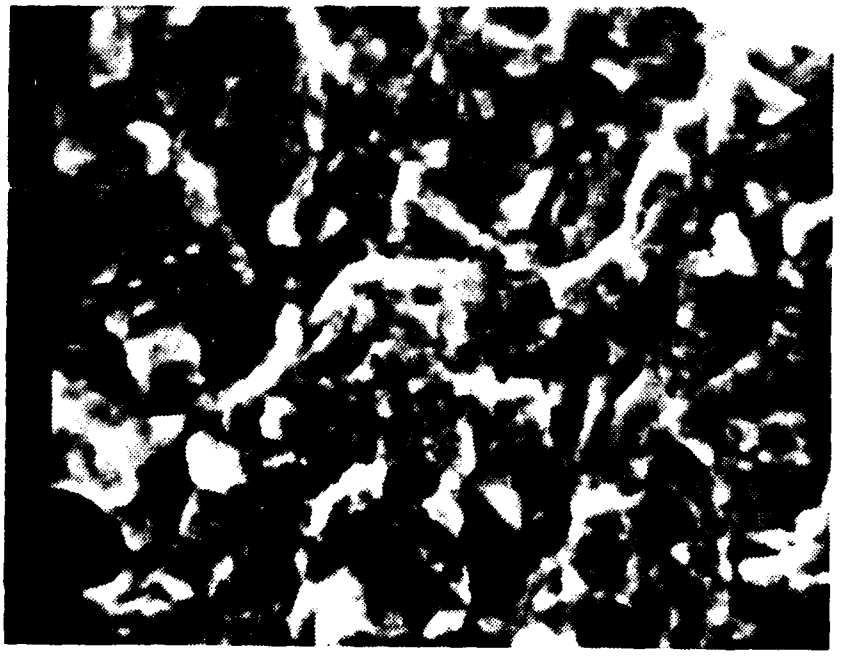

Figure 36. Fractograph of 550 C Rolled Material Fracture Surface After Hardening Treatment 250-IT. This surface indicates primarily a brittle failure. 2000X

Figure 37. Fractograph Of Standard 52100 After Hardening Treatment 300-IT. This increased brittleness was due to temper embrittlement. 2000X

Figure 38. Fractograph Of 550 C Rolled Material After Hardening Treatment 300-IT. The large dimples indicate increased ductility. 2000X

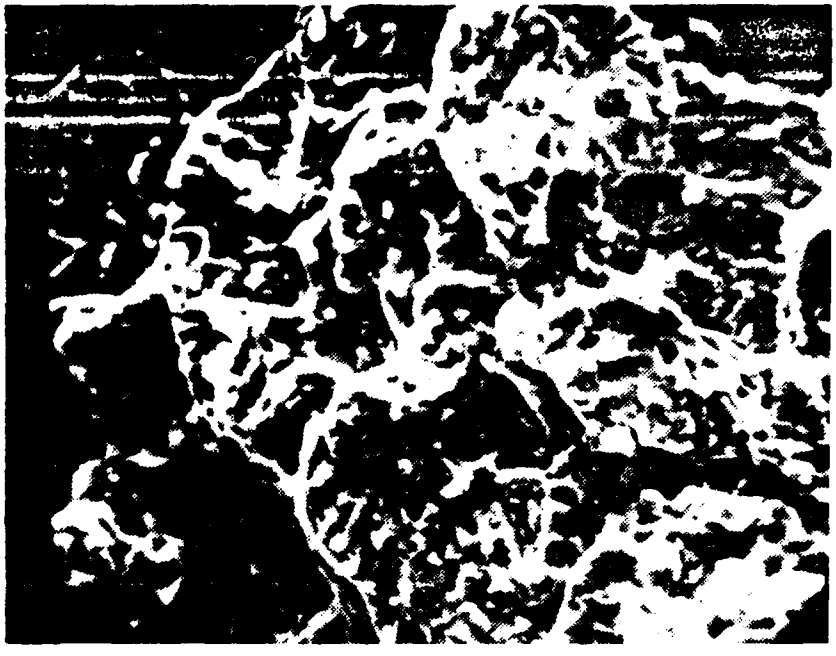

Figure 39. Fractograph Of 650 C Rolled Material After Hardening Treatment 300-IT. The dimples and tear ridges indicate improved ductility. 2000X

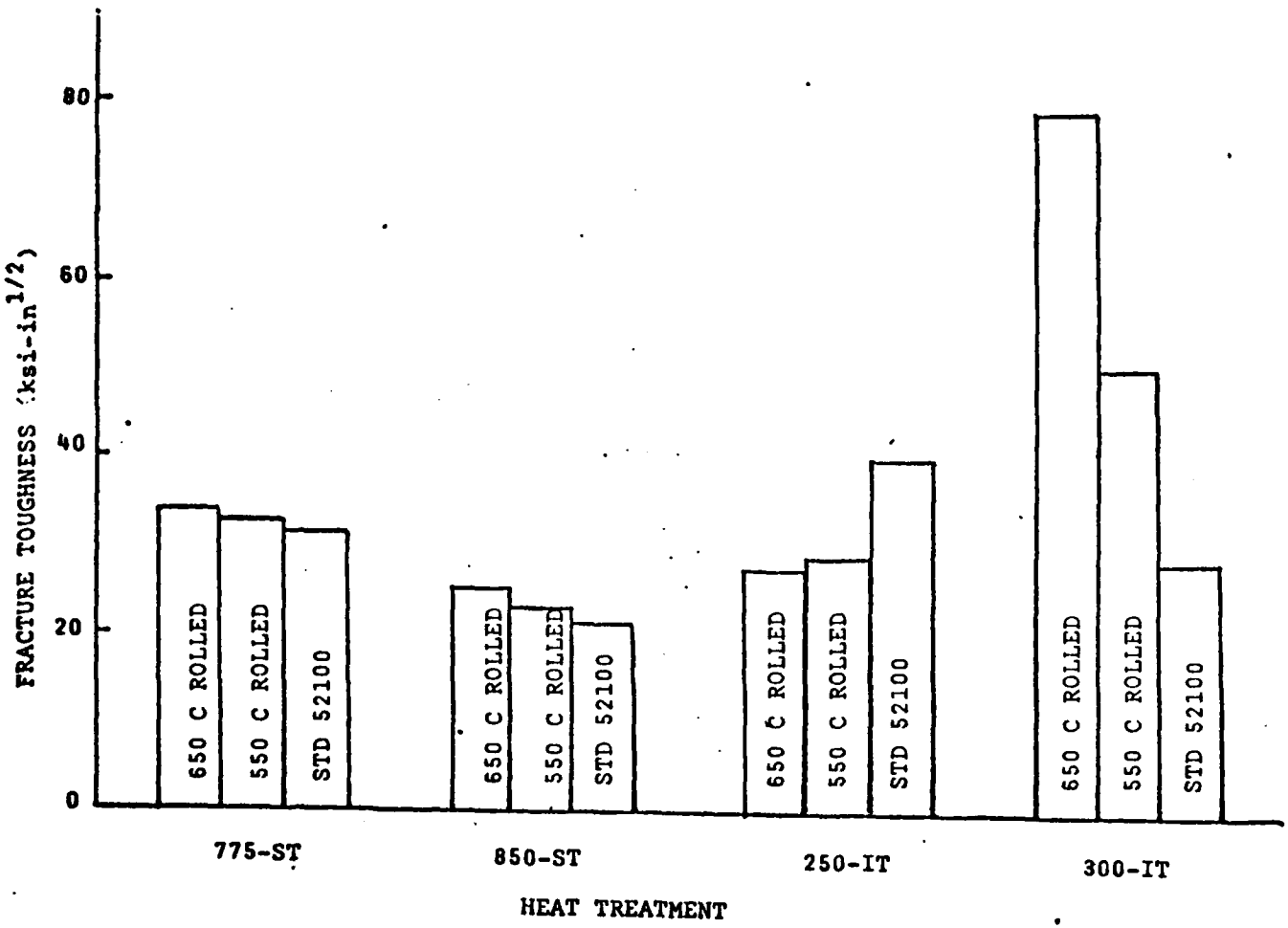

Figure 40. Fracture Toughness vs. Heat Treatment. This bar graph shows the toughness values attained for the various materials after different heat treatments.

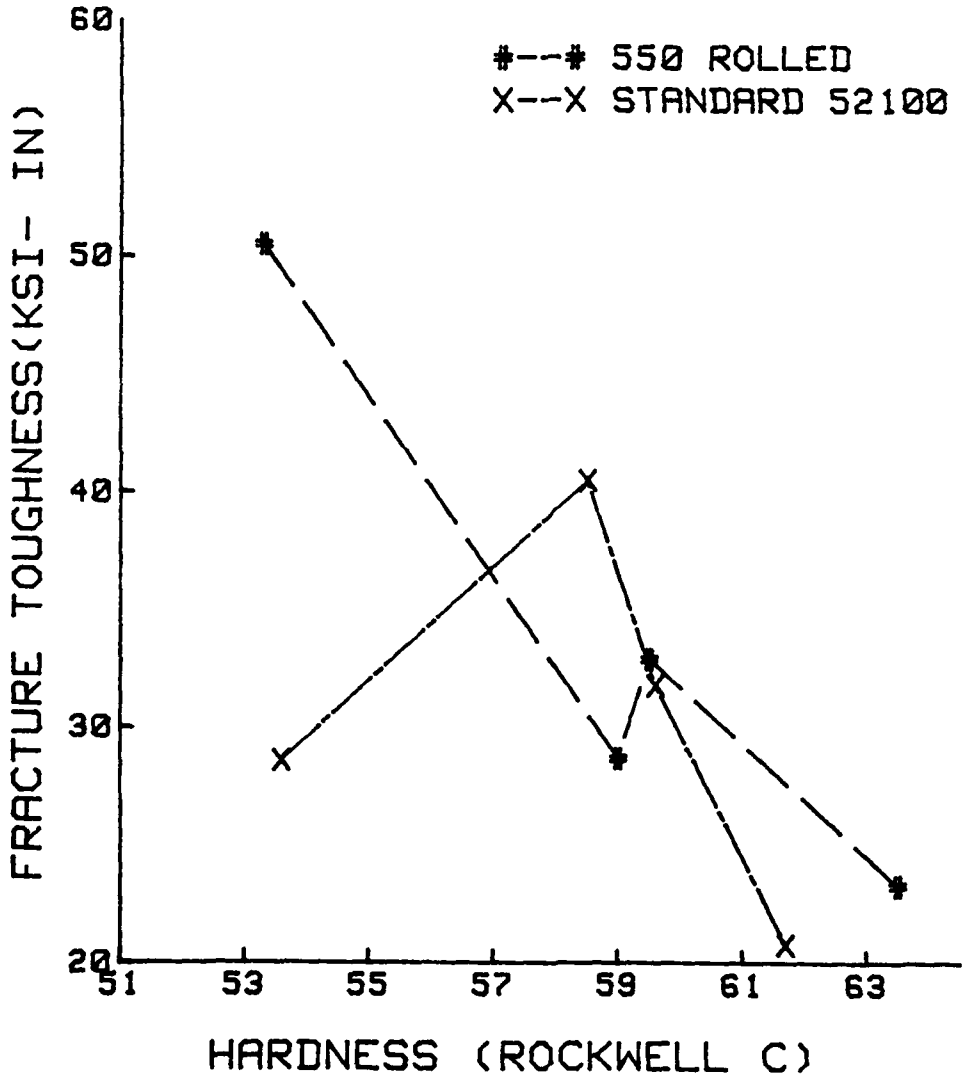

Figure 41. Fracture Toughness vs. Hardness For The Standard 52100 And The 550 C Rolled Material.

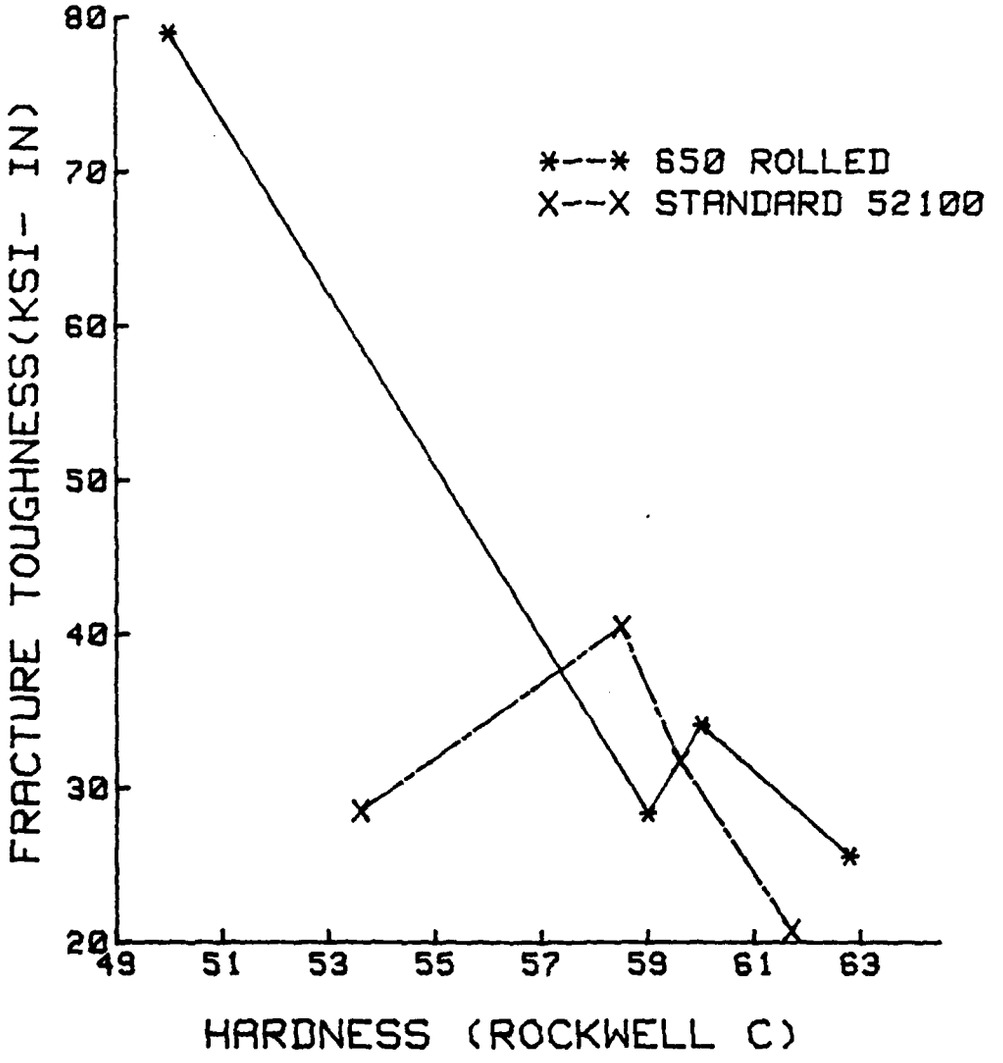

Figure 42. Fracture Toughness vs. Hardness For The Standard 52100 And The 650 C Rolled Material.

LIST OF REFERENCES

1. Taylor, J.L., Fracture Toughness of Selected ULTRA High Carbon Steels, M.S. Thesis, Naval Postgraduate School, Monterey, California 1979.

2. ASTM Committee E-24 on Fracture Testing, 1978 Annual Book of ASTM Standards, Part 10, American Society for Testing and Materials, 1978.

3. Eschmann, P., Hasbargen, L., and Weignad, P., Ball and Roller Bearings, Heyden, 1958.

4. Metals Handbook, 9th ed., v. 1, p.606, American Society for Metals, 1978.

5. Bisson, E. E., and Anderson, W. J., Advanced Bearing Technology, National Aeronautics and Space Administration, 1964.

6. Morrison, T. W., Walp, H. O., and Remorenko, R. P., "Materials in Rolling Element Bearings for Normal and Elevated Temperatures," ASLE, v.2, no. 1, April 1959, p. 129-146.

7. Kar, R., Horn, R. M., and Zackay, V. F., "The Effect of Heat Treatment on Microstructure and Mechanical Properties in 52100 Steel," Metallurgical Transactions, v. 10A, pp. 1711-1717, November 1979.

8. Reed-Hill, R. E., Physical Metallurgy Principles, Van Nostrand, 1964.

9. Third Semi-annual Progress Report to Advanced Progress Research Agency under grant DAHC-15-73-G15, Superplastic Ultra High Carbon Steels, Stanford University Press, by O.D. Sherby and others, February 1975.

10. Goesling, W. H., Ballistic Characterization of Ultra High Carbon Steel, M.S. Thesis, Naval Postgraduate School, Monterey, California 1977.

11. Powe, D., and Hamilton, D. R., The Microstructural, Mechanical and Ballistic Characterization of Ultra High Carbon Steel, M.S. Thesis, Naval Postgraduate School, Monterey, California 1977.

12. Phillips, J. W., and Martin, R. R., Ballistic Performance Shear Band Formation and Mechanical Behavior of Thermo-Mechanically Processed Ultra-High Carbon Steel, M.S. Thesis, Naval Postgraduate School, Monterey, California 1978.

13. Hillier, R., Evaluation of Superplastic Ultra-High Carbon Steel As Armor Plate For Critical Component Protection, M.S. Thesis, Naval Postgraduate School, Monterey, California 1979.

14. Chung, I., The Fatique And Fractographic Characteristics of AISI 52100 Steel, M.S. Thesis, Naval Postgraduate School, Monterey, California 1979

15. Sherby, O. D., and others, "Development Of Fine Spheroidized Structures by Warm Rolling of High Carbon Steels," Transactions Of The American Society For Metals, v. 62, 1969.

16. Second Annual Report to Advanced Projects Research Agency Under Grant DAHC-15-73-C15, Superplastic Ultra-High Carbon Steels., Stanford University Press, by O.D. Sherby and B. Walsner, August, 1975.

17. Lake, R. L., Answers To Some Questions About Fracture Mechanics, Kaiser Aluminum and Chemical Corporation Center for technology, 1975.

18. Tom, T., D.E. Microstructural Variables and Fracture Toughness of High Strength Mo and Mo-Ni Steels, D.E. Thesis, University of California, Berkeley, 1973.

19. Hertzberg, R. W., Deformation and Fracture Mechanics of Engineering Materials, Wiley, 1976.

20. Liu, H. W., "Fracture Toughness Testing And Its Application," ASTM Special Technical Publication 381., 1965.

21. Heald, P.T., Spink, G. M., and Worthington, P. J., "Post Yield Fracture Mechanics," Materials Science and Engineering v. 10, 1972.

22. Ogilvie, R. E., "Retained Austenite By X-ray," Metallurgical Transactions, v. , pp. 60-61, 1979.

INITIAL DISTRIBUTION LIST

		No. Copies
1.	Defense Documentation Center Cameron Station Alexandria, Virginia 22314	1
2.	Library, Code 0142 Naval Postgraduate School Monterey, California 93940	2
3.	Department Chairman Code 69Mx Department of Mechanical Engineering Naval Postgraduate School Monterey, California 93940	1
4.	Assoc Professor T.R. McNelly Code 69Mc Department of Mechanical Engineering Naval Postgraduate School Monterey, California 93940	5
5.	LT Jeffrey F. McCaulev, USN 1123 South 5th Edmonds, Washington 98020	1
6.	Professor Oleg D. Sherby Department of Material Science & Engineering Stanford University Stanford, California 94305	1